



Review

Nanoantibiotics Based in Mesoporous Silica Nanoparticles: New Formulations for Bacterial Infection Treatment

Elena Álvarez ^{1,2}, Blanca González ^{1,2} , Daniel Lozano ^{1,2} , Antonio L. Doadrio ¹, Montserrat Colilla ^{1,2,*} and Isabel Izquierdo-Barba ^{1,2,*}

¹ Departamento de Química en Ciencias Farmacéuticas, Universidad Complutense de Madrid, Instituto de Investigación Sanitaria, Hospital 12 de Octubre i+12, Plaza Ramón y Cajal s/n, 28040 Madrid, Spain; elealvar@ucm.es (E.Á.); blancaortiz@ucm.es (B.G.); danlozan@ucm.es (D.L.); antoniov@ucm.es (A.L.D.)

² CIBER de Bioingeniería, Biomateriales y Nanomedicina, CIBER-BBN, 28040 Madrid, Spain

* Correspondence: mcolilla@ucm.es (M.C.); ibarba@ucm.es (I.I.-B.); Tel.: +34-919341870 (M.C. & I.I.-B.)

Abstract: This review focuses on the design of mesoporous silica nanoparticles for infection treatment. Written within a general context of contributions in the field, this manuscript highlights the major scientific achievements accomplished by professor Vallet-Regí's research group in the field of silica-based mesoporous materials for drug delivery. The aim is to bring out her pivotal role on the envisage of a new era of nanoantibiotics by using a deep knowledge on mesoporous materials as drug delivery systems and by applying cutting-edge technologies to design and engineer advanced nanoweapons to fight infection. This review has been divided in two main sections: the first part overviews the influence of the textural and chemical properties of silica-based mesoporous materials on the loading and release of antibiotic molecules, depending on the host–guest interactions. Furthermore, this section also remarks on the potential of molecular modelling in the design and comprehension of the performance of these release systems. The second part describes the more recent advances in the use of mesoporous silica nanoparticles as versatile nanoplatforams for the development of novel targeted and stimuli-responsive antimicrobial nanoformulations for future application in personalized infection therapies.

Keywords: nanoantibiotics; mesoporous silica nanoparticles; targeted therapies; stimuli-response; infection treatment; metal ions



Citation: Álvarez, E.; González, B.; Lozano, D.; Doadrio, A.L.; Colilla, M.; Izquierdo-Barba, I. Nanoantibiotics Based in Mesoporous Silica Nanoparticles: New Formulations for Bacterial Infection Treatment. *Pharmaceutics* **2021**, *13*, 2033. <https://doi.org/10.3390/pharmaceutics13122033>

Academic Editor: Ildiko Badea

Received: 20 October 2021

Accepted: 24 November 2021

Published: 29 November 2021

Publisher's Note: MDPI stays neutral with regard to jurisdictional claims in published maps and institutional affiliations.



Copyright: © 2021 by the authors. Licensee MDPI, Basel, Switzerland. This article is an open access article distributed under the terms and conditions of the Creative Commons Attribution (CC BY) license (<https://creativecommons.org/licenses/by/4.0/>).

1. Introduction

Infections associated with bone implants are one of the most severe and overwhelming threats to society today [1,2]. The implant surface constitutes a perfect environment for bacterial adhesion, growth and colonization [3]. In addition, the wear produced by the micromotions of these bone prostheses provokes the release of residues that elicit inflammation local, which provides an ideal place for the appearance of infections [4]. Nowadays, although significant improvements in prophylaxis and aseptic surgical procedures have remarkably decreased the prevalence of implant infections, the infection rates remain in the 1–2% range [5]. Moreover, the reinfection rate following revision surgical procedures are also extremely elevated (ca. 33%) [6], which increases the expenses associated with the treatment. These bone implant infections are caused by pathogens such as *Staphylococcus aureus* [7], whose resistance mechanisms make it resilient and invincible [8]. Among the difficulties of eradicating implant-associated infections, biofilm formation is the most challenging and outstanding one, since it provides the bacteria with a perfect environment for longstanding survival [9,10]. The action of antibiotics is prevented by these biofilms, which serve as an impenetrable physical barrier [11]. In addition, the bacteria existing into the biofilm are especially pathogenic due to their phenotypic diversity, which confers resistance to antimicrobial treatment, making the dose of drugs to be administered up to 1000 times greater than that necessary for their planktonic phenotype [9,12]. Another major

concern is that biofilm causes irreversible damage, provoking bone resorption, due to both the direct bacteria's intrinsic aggressiveness and the indirect associated inflammatory processes [13,14].

Once an infection is detected in an orthopedic prosthesis, the major hurdle is its complete elimination from the affected area, including the implant and the adjacent necrotic regions. Usually, antibiotics are massively administered to the patient during long-time hospitalization periods. Unfortunately, most of the cases require a second surgical procedure to replace the infected prosthesis at the same time that a local treatment using antibiotic loaded poly(methylmethacrylate) beads is applied [15]. Nonetheless, the total eradication of the infected areas is a difficult task, and latent bacteria are responsible for recurrent and antimicrobial resistant infections. The high morbidity and patient suffering, as well as the associated economic burdens for the national healthcare systems, have motivated the scientific community to devote much research effort to the development of alternative therapies able to circumvent the limitations of those used nowadays [16]. Currently, there is not any consensual and efficient therapy for the management of bone implant infection; there is an urgent need to find a solution to this changeling problem [15,17].

New therapeutic advancements should be aimed at avoiding the need of implant removal and replacement by means of the in situ treatment of the infected region, in a localized manner and with the greatest possible specificity. Nanotechnology has entered into this arena, providing powerful tools to design and engineer nanoparticles as nanoweapons to fight bacterial infection much more effectively than conventional antimicrobial treatments. These nanoparticles are envisioned as targeted nanomedicines for local treatments, achieving higher antimicrobial effect at low doses, and therefore reducing toxicity and side effects. Among nanoparticles, there are those with inherent antimicrobial properties, such as metal (Ag, Au, etc.) and metal oxide (ZnO, CuO, TiO₂, etc.) nanoparticles [18–20] and nanoparticles acting as nanocarriers of antimicrobial agents, the so-called nanoantibiotics [21,22].

Among nanocarriers, mesoporous silica nanoparticles (MSNs) are one of the most promising ones due to their interesting structural and textural properties, which allow them to host a wide range of different therapeutic cargoes for drug delivery in different biomedical applications, including cancer, osteoporosis and infection, among others [23–35].

In the field of bone infection, professor Vallet-Regí and co-workers envisaged the design and development of advanced nanoantibiotics as a challenging scientific scenario, starring three main actors: bacteria, antimicrobials and MSNs (Figure 1). Firstly, bacteria, which are present in bone implant infection, either in planktonic state or forming highly resistant biofilms, must be eradicated in situ in a localized fashion, to avoid the need of surgical procedures to remove and replace the infected prosthesis. On the other hand, antimicrobials (including antibiotics alone or in combination with metal ions) should be locally delivered at the infected target site at small doses with high specificity, which would increase the antimicrobial efficacy and reduce the risk of harmful side effects in healthy organs, tissues and cells. This goal can be accomplished by using nanocarriers able to load, protect and transport antimicrobials to the target (bacteria and/or biofilm). Once there, the nanocarriers steadily release antimicrobials in response to certain internal or external stimuli. Among nanocarriers, MSNs emerged as the third actor that fulfils all of these requirements. Thus, innovative cutting-edge technologies are being applied to design and engineer innovative targeted stimuli-responsive antimicrobials delivery MSNs-based nanosystems.

This review aims to provide a comprehensive overview of the most recent scientific advances carried out by professor Vallet-Regí's research group in the field of MSNs for bacterial infection treatment [36]. First, the role of silica-based mesoporous materials as drug delivery devices of antimicrobial agents is described. The influence of the textural properties (pore diameter, surface area and pore volume), chemical nature of the surface of these materials and host–guest interactions, on the loading and release kinetics of different antibiotics is revised. Furthermore, the potential of molecular modelling in the design

of these controlled delivery devices and a deep comprehension on their performance as release systems of antibiotics of different families is also described. Finally, the more recent scientific approaches aimed to design and develop advanced nanoantibiotics for future applications in personalized therapies are tackled.

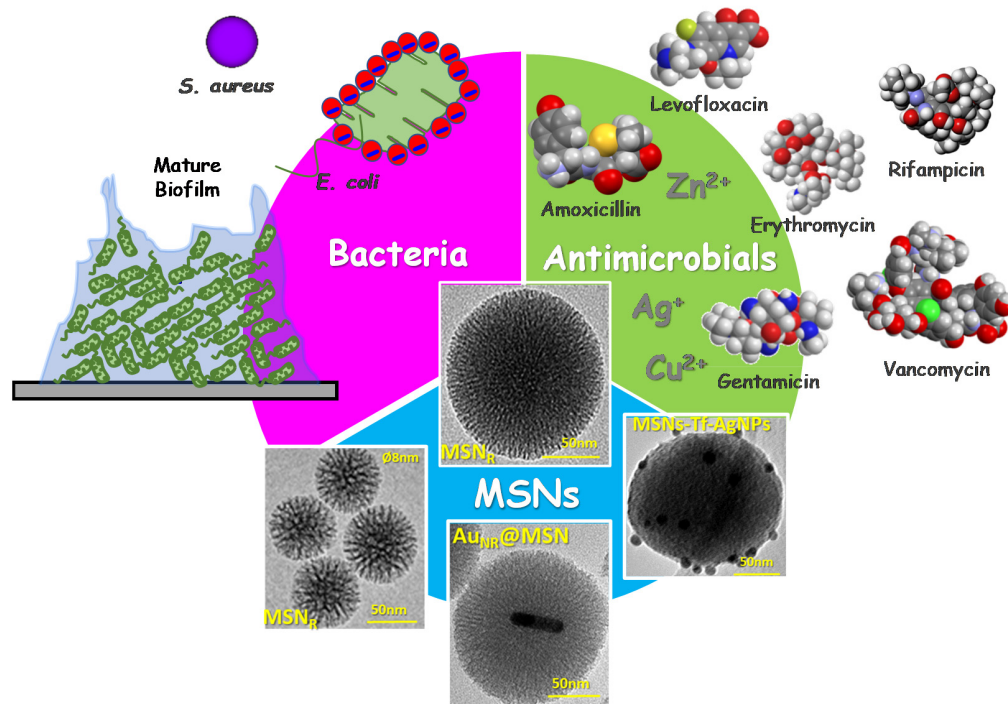


Figure 1. Schematic depiction of the three main actors starting in the innovative scientific approaches developed by professor Vallet-Regí's research group in the design and engineering of nanoantibiotics for infection treatment: bacteria (in planktonic state or biofilms), antimicrobial agents (including antibiotics alone or in combination with metal ions) and mesoporous silica nanoparticles (MSNs). MSN_R: Radial mesoporous silica nanoparticles; Au_{NR}@MSN: gold nanorods@mesoporous silica nanoparticles; MSN-Tf-AgNPs: mesoporous silica nanoparticles decorated with transferrin and silver nanoparticles.

2. Engineering Mesoporous Materials as Antimicrobial Delivery Systems

The pioneering research on MCM-41 material as a controlled delivery system of ibuprofen [37], an anti-inflammatory used as a model drug, inspired the design and engineering of an important number of silica-based mesoporous matrices to host diverse antimicrobial agents such as antibiotics [26,28–30,38–41]. The reasons that account for the high impact of mesoporous materials in the field of controlled drug delivery rely on their distinctive structural (ordered pore structure), textural (narrow pore size distributions, large surface areas and high surface volumes) and chemical (high density of silanol groups that allows the covalent grafting of organic groups) properties, which are pivotal factors in the performance of these systems during the loading and release of drug molecules (Figure 2) [31,42–44].

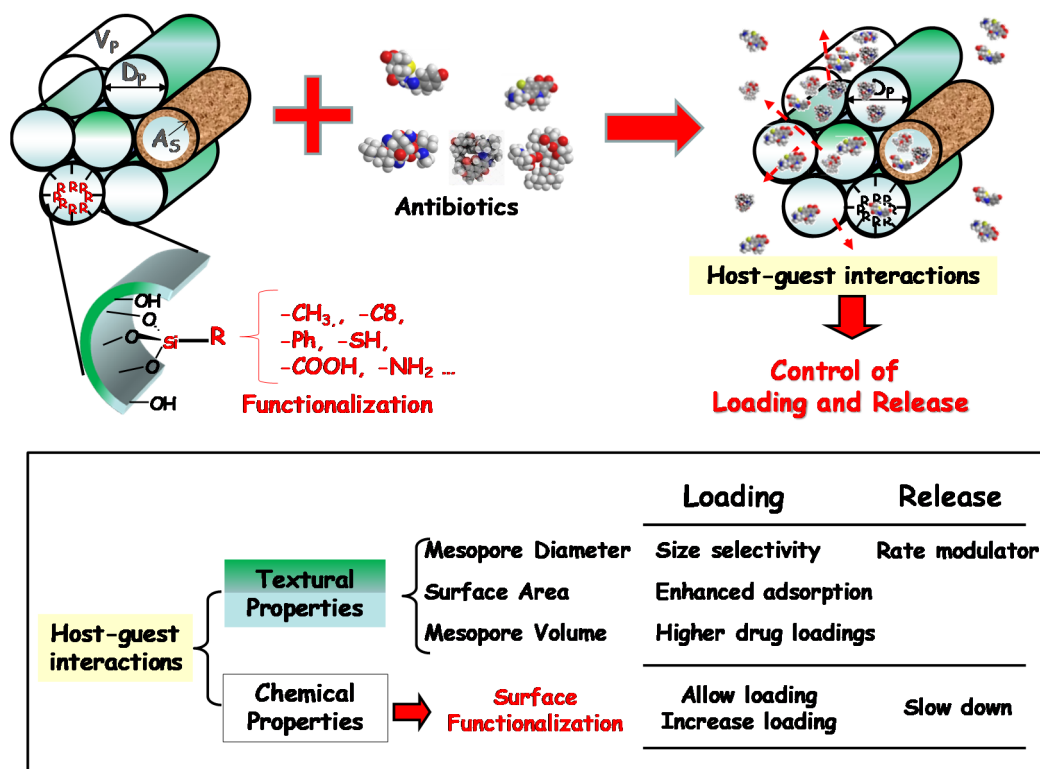


Figure 2. Influence of the textural and chemical properties of the silica-based mesoporous matrices in their performance as drug delivery systems.

The pore diameter restricts the maximum size that the drug molecules can have to enter the channels of the mesoporous material, therefore being a size-selectivity parameter during the drug loading process. This parameter also limits the diffusion of the cargo molecules to the delivery medium, therefore acting as a release rate modulator. The loading of molecules into the mesopores depend on the adsorptive capacity of the host and consequently on the surface area of the matrix. Thus, large surface areas in the host increase the contact time with the guest molecule, which results in higher amounts of loaded drug. Finally, the pore volume may increase the amount of loaded drug if pore filling is accomplished, which involves an increase in the drug–drug interactions inside the mesoporous cavities [42,43].

With respect to the chemical properties, the amorphous silica surface is covered by siloxane bridges and silanol groups. The magnitude of the silanol number, that is, the number of OH groups per unit of surface area, is considered to be a physico-chemical constant when the surface is hydroxylated to the maximum degree. This constant has the numerical value of $4.9 \text{ OH}/\text{nm}^2$ (arithmetical mean) and is known in the literature as the Kiselev–Zhuravlev constant [45,46]. These silanol groups provide many opportunities to modulate the host–guest interactions [47]. Thus, when pure silica mesoporous matrices are used, their interaction with the drug molecules would take place through weak interactions, such as Van der Waals forces or hydrogen bonds. Nevertheless, it is feasible to functionalize such silanol-containing mesoporous groups by covalently anchoring diverse organic groups, which leads to a full family of organic–inorganic hybrid materials [42,48–50]. The two main approaches used to functionalize silica mesoporous matrices are the post-synthesis method, also known as silanization or grafting, and the one-pot synthesis or co-condensation route. The post-synthesis method is generally carried out under anhydrous conditions by reaction of organosilanes of the $(\text{R}'\text{O})_3\text{SiR}$ type, with the free silanol groups of the host matrix. This is a versatile method that allows the selective functionalization of either the external surface of the mesopore, when the process is performed before the surfactant removal, or the entire

silica surface, i.e., the inner and external mesoporous surface, when the procedure is carried out once the surfactant has been extracted. Such functionalization provokes a decrease in the textural properties of the resulting material, due to presence of organic moieties into the mesopore voids, which is accompanied by an increase in the wall thickness. On the other hand, the co-condensation route is a one-step method comprising the simultaneous hydrolysis and condensation reactions of both silica and organosilica precursors in the presence of a surfactant as a structure-directing agent. In this last method, there is a more homogeneous distribution of the organic functions covering the entire silica surface, but there is an upper functionalization threshold above to avoid the disorder of the mesoporous structure [48].

Functionalization of mesoporous matrices permits a precise modulation of drug loading and release kinetics [43], as a result of the different host–guest interactions via electrostatic attractive forces, hydrophilic–hydrophobic interactions or electronic interactions [47,51,52].

Figure 3 shows the drug release curves of three antibiotics of different chemical nature, namely levofloxacin (LEVO), gentamicin (GM) and rifampicin (RIF) from pure-silica (MSN) and amino-modified (MSN-NH₂) MSNs [53]. In such research work, MSN-NH₂ was used as a model nanoplatform, since amino-functionalization of mesoporous matrices are widely reported in the literature [44]. The different release profiles observed in each case account for the different nature of the host–guest interactions, and also to the chemical properties of the antibiotic molecule. For comparative purposes, the experimental data were fitted to a typical diffusion first order release kinetics model [54]. In the case of LEVO, there is an initial burst effect followed by a more sustained release; moreover, there is a partial antibiotic retention in the pure silica MSN (Figure 3A). This behavior is in good agreement with the strong attracting interactions via hydrogen bonds of LEVO molecules and the silanol groups present in bare silica MSN, as previously reported [55–57]. On the contrary, the repulsive interactions of the antibiotic molecule with protonated amino groups in the host matrix at physiological conditions would trigger the total antibiotic release from LEVO loaded in MSN-NH₂. Concerning GM, despite the different existing host–guest interactions, the high solubility of this molecule is the predominant factor that provokes the total antibiotic release from both nanomaterials with similar profiles (Figure 3B). Finally, in the case of RIF, the lack of burst effect and noticeable drug retention can be mainly explained by the low solubility and relatively high molecular size of such an antibiotic [58].

The above described research study reveals that the release of antibiotics of different families from mesoporous matrices strongly depends both on the chemical properties of the drug itself and the host–guest-interactions. In this sense, molecular modelling has been revealed as a powerful tool to gain deeper comprehension of these aspects, bringing up the possibility to understand, and even predict, the loading and release performance of these systems [59]. Actually, it was back in 1996 when Gusev et al., published a molecular model for MCM-41 mesoporous material [60], which was considered the “molecule of the month” in April of 1998 by Bristol University. Molecular modeling allows creating 3D models, for both the mesoporous matrix and the drug, which are then used for the docking calculations to predict the preferred orientation of the drug (ligand) into the mesoporous matrix (the receptor) to form a stable complex, i.e., minimal energy configuration [61]. Table 1 shows a selection of some representative antibiotics that have been loaded into pure-silica mesoporous matrices and then released in a controlled fashion by Vallet-Regí’s and others’ research groups. The results derived from molecular modeling and docking studies are also displayed (unpublished data).

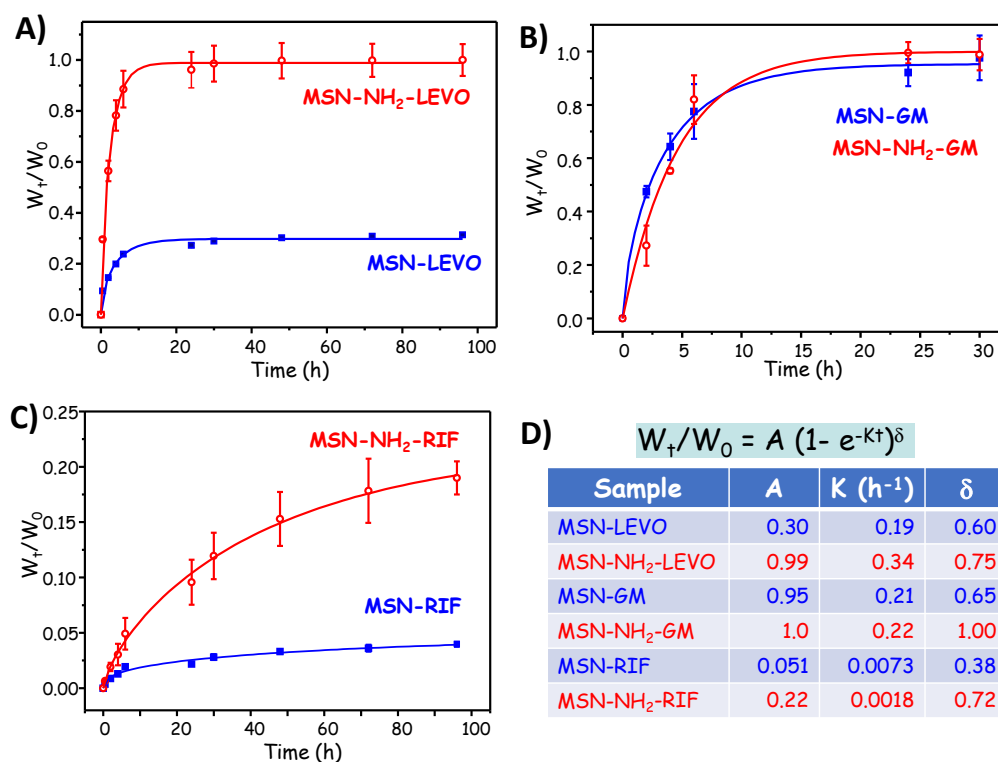
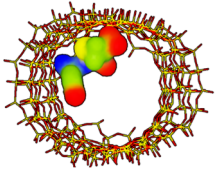
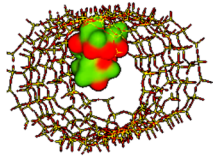
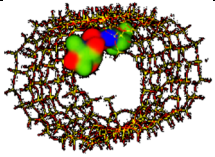
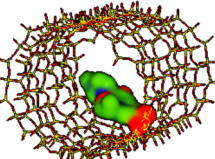
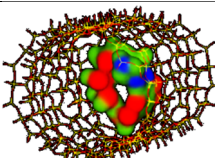
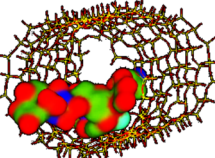


Figure 3. Drug release curves of three antibiotics: (A) levoﬂoxacin (LEVO); (B) gentamicin (GM); and (C) rifampicin (RIF), from pure-silica (MSN) and amino-modified (MSN-NH₂) MSNs. (D) Kinetic parameters derived from the fit of the experimental data to theoretical kinetic model using the equation $W_t/W_0 = A(1 - e^{-kt})^\delta$, where W_t is the amount of antibiotic released at t time, W_0 is the initial amount of loaded drug, A is the maximum antibiotic release at infinite time, k is the release kinetic constant and δ is a dimensionless non-ideality parameter. Adapted with permission from Aguilar et al. [53], *Micropor. Mesopor. Mat.*, published by Elsevier, 2021.

To design the appropriate 3D model for the pure-silica mesoporous matrix, the different textural properties derived from N₂ adsorption porosimetry measurements have to be determined. Among them, pore diameter, which is the release rate modulator, as above discussed (see Figure 2), is of foremost relevance. On this regard, MCM-41- and SBA-15-type mesoporous materials have been the most widely used host matrices for drug delivery proposes. Both materials display 2D-hexagonal structure with honeycomb arrangements of mesopores, but with different pore size, being 9–30 nm for SBA-15 and 2–10 nm for MCM-41. In addition, SBA-15-type structure contains interconnecting micropores; however, they were not taken into account to create the 3D model, since the drugs cannot penetrate into this small-size microporous channel. Accordingly, MCM-41 was used as the simplest and most useful model for these studies, and, taking into account the average data found in the literature, mesopore dimensions of 3.0 nm in diameter and 4.0 nm in length were fixed for the computational calculations.

The different electrostatic potentials maps of the different antibiotics included in Table 1 allowed predicting the functional group of the drug molecule interacting with the native silica matrix. In such maps, the atomic regions rich in electrons are typically represented in red color, whereas the electron-deficient regions are displayed in blue. In addition, other colors, such as green and yellow, are uniformly distributed and represent the covalent bonds or electron delocalization of π bonds.

Table 1. Summary of selected representative antibiotics that have been hosted into different pure-silica mesoporous matrices for controlled delivery proposes. Results derived from molecular modelling and docking studies of MCM-41-antibiotic host–guest interactions, carried out using Hex 8.0 software, are also shown (unpublished data).

Antibiotic/Host Matrix/ Antibiotic Family	Docking *	Computed Properties Drug **	H-Bonds Count **
Amoxicillin MCM-41 [62] SBA-15 [63] Semisynthetic penicillin	 $E_{\text{complex}} -227.65 \text{ kJ/mol}$	$M_w = 365.4 \text{ amu}$ $XlogP3 = -2.0$ Length = 10.63 Å Width = 7.90 Å	Donor drug 4 Acceptor drug 7 Complex 5
Erythromycin MCM-41 [64], MCM-41-Ti [65], SBA-15 [66], LP-Ia3d [67] Broad-spectrum macrolide	 $E_{\text{complex}} -315.45 \text{ kJ/mol}$	$M_w = 733.9 \text{ amu}$ $XlogP3 = 2.7$ Length = 14.01 Å Width = 9.70 Å	Donor drug 5 Acceptor drug 14 Complex 1
Gentamicin MCM-41 [68], SBA-15 [69] Broad-spectrum aminoglycoside	 $E_{\text{complex}} -256.08 \text{ kJ/mol}$	$M_w = 477.6 \text{ amu}$ $XlogP3 = -4.1$ Length = 14.10 Å Width = 8.90 Å	Donor drug 8 Acceptor drug 12 Complex 6
Levofloxacin MCM-41 [70], SBA-15 [71] Broad-spectrum, third-generation fluoroquinolone	 $E_{\text{complex}} -241.96 \text{ kJ/mol}$	$M_w = 361.4 \text{ amu}$ $XlogP3 = -0.4$ Length = 14.20 Å Width = 7.50 Å	Donor drug 1 Acceptor drug 8 Complex 1
Rifampicin MCM-41 [72], MSNs [73] Semisynthetic amycolatopsis rifamycinica	 $E_{\text{complex}} -349.59 \text{ kJ/mol}$	$M_w = 822.9 \text{ amu}$ $XlogP3 = 4.9$ Length = 14.50 Å Width = 11.50 Å	Donor drug 5 Acceptor drug 15 Complex 5
Vancomycin SBA-15 [59] Branched tricyclic glycosylated peptide	 $E_{\text{complex}} -486.39 \text{ kJ/mol}$	$M_w = 1449.2 \text{ amu}$ $XlogP3 = -2.6$ Length = 19.74 Å Width = 18.70 Å	Donor drug 19 Acceptor drug 26 Complex 4

* MCM-41 host matrix is essentially composed of negative formal charges; in drugs, red represents negative formal charges while the blue color represents positive formal charges, as shown in the electrostatic potential color scale: ; E_{complex} is the electrostatic potential energy in the model complex, where MCM-41 was used as receptor and the antibiotic as ligand. ** XlogP3 (for the fast calculation of partition coefficient, logP), donor and acceptor drug H-bonds have been obtained from PubChem DataBank. Complex H-bonds have been obtained from Hex 8.0 docking software.

Figure 4 shows representative examples of the application of these 3D molecular models in different MCM-41-antibiotic release systems investigated by our research group. If we observe the electrostatic potential density maps for amoxicillin (Figure 4A) and

vancomycin (Figure 4B), both antibiotics exhibit regions of negative charges, and others of positive charge. In this case, the host–guest electrostatic attracting interactions between the negatively-charged silica surface and the positive regions in the antibiotic will govern drug loading and release behaviors. Such interactions are relatively weak and the magnitude of their extension depends on the size of the antibiotic. Thus, amoxicillin is small enough to penetrate into the mesoporous channels and orientates to procure interaction of its positive charged regions with the negatively charged silica surface, therefore reducing the repulsive forces between electron-rich areas (Figure 4A). On the contrary, vancomycin is too large to penetrate into the mesopore channel; therefore, it remains located on the outside of the channels, i.e., at the pore entrance, with the low electron density regions orientated to procure interaction with the negatively charged surface of the silica, as shown in Figure 4B. This predictive study agrees with the experimental results derived from loading and release assays results reported by Doadrio and coworkers [59,63].

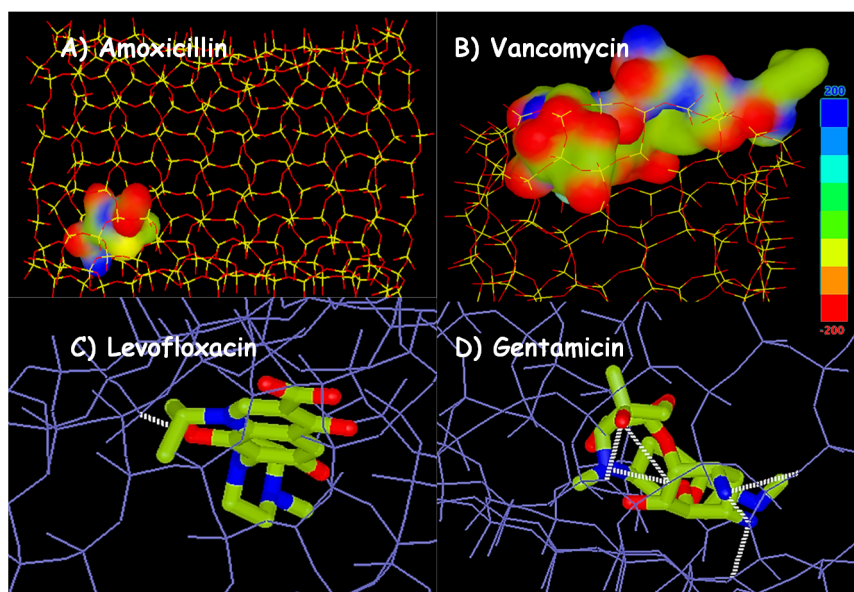


Figure 4. Molecular 3D models carried out with Hex 8.0 software. Electrostatic potential density maps for (A) amoxicillin and (B) vancomycin forced to penetrate into a 3.0×4.0 nm silica mesopore. Molecular modelling interactions studies where pure silica matrix model was used as receptor and (C) levofloxacin and (D) gentamicin as ligands.

On the other hand, hydrogen bonding host–guest interactions can be also established. These forces are stronger than electrostatic ones, and therefore they significantly influence the antibiotic release rate from pure-silica mesoporous material. Thus, the greatest the number of hydrogen bonds in the complex the slowest the release rate, as demonstrated by Doadrio et al. [74]. As representative examples, Figure 4C,D illustrate the 3D molecular models representing the hydrogen bonding that can be established in the MCM-41-antibiotic complexes for levofloxacin and gentamicin, respectively.

However, to fully understand the release behavior of the different antibiotics, their solubility in the aqueous medium mimicking physiological conditions cannot be overruled. Thus, the higher the solubility, the faster the release rate, as previously reported [74]. The XlogP3 values, which are closely related to the solubility, for the different investigated antibiotics are displayed in Table 1. The smaller the XlogP3 value, the higher the solubility, and therefore the faster the release rate and the greater the amount of released drug. Thus, such antibiotics showing negative XlogP3 values account for the optimal solubility in the aqueous medium.

In summary, the two parameters that mostly influence antibiotic release kinetic profiles from pure silica mesoporous matrices are the possibilities for hydrogen bonding

formation and the drug solubility. For instance, experimental studies carried out by Aguilar-Colomer et al. [53] using MSNs as levofloxacin and gentamicin delivery nanodevices revealed that gentamicin, which is much more soluble in water ($X_{\log P3} = -4.1$) than levofloxacin ($X_{\log P3} = -0.4$), is more quickly released despite exhibiting a higher number of hydrogen bonds (6 hydrogen bonds) compared to the unique H-bond in the case of levofloxacin (Figure 4C,D, Table 1) [53].

3. A New Era of the Nanoantibiotics

In the last decade, the concept of nanoantibiotic as delivery-carrier is beginning to emerge as a very powerful therapy in the field of bacterial infection [22]. A drug delivered through nanoparticulate forms can release and specifically connect to cellular and intracellular targets, provoking much greater antimicrobial efficiency compared to the antibiotic isolated [75]. Moreover, it is a fundamental tool in the design of localised therapies, delivering large quantities of antimicrobials to the site of infection, achieving more effective therapies with lower doses, and eliminating many of the side effects. Among the different nanocarriers that can be used, the MSNs nanoparticles have been the focus of development in professor Vallet-Regí's group [23–25,31,32,43,76,77]. The main strengths of MSNs as nanocarriers are their high biocompatibility and chemical stability as well as their high loading capacity, thanks to the characteristic pore lattice, and their easy functionalisation due to the presence of silanol groups. Moreover, these nanoparticles can be easily synthesized on a large scale showing a wide variety of morphologies, pore sizes, pore-lattices and surface functionalities using different strategies, thus demonstrating the great versatility of these nanosystems [31,32,42,44,47,78,79]. In this sense, MSNs can be compared to a RUBICK's cube in which each face represents one aspect to be modified in these nanosystems, such as targeting, stealthy, peptide/protein loading, stimuli response elements, drug/ions loading and structural characteristics. Thanks to its enormous versatility and numerous positions, this "RUBICK's cube" will give rise to multiple nanosystems to treat of different pathologies, including the bacterial infection (Figure 5). This section aims to give an overview of the main advances of these nanoparticles in the treatment of infection that have been made in professor Vallet-Regí's group. First, it will show how MSN nanosystems are ideal nanocarriers of different antibiotics and their direct effect on the biofilm. Second, their targeting capacity towards the bacteria and the biofilm will be discussed. Third, their capacity to host different antimicrobial agents in the same nanosystem and, finally, the design of MSN-based stimuli-responsive nanosystems, will be tackled.

3.1. Antimicrobial Doses as Key Factor for Custom-Made Therapies

A great number of studies have proposed multifunctional MSNs as release systems of antimicrobials for infection therapy [2,26,29,30,40,77]. In general, the antibacterial and/or antibiofilm effect of the nanosystems has been investigated as a whole, i.e., evaluating the combined effect of the different elements in the nanopatform. Nonetheless, poor attention has been paid to the sole evaluation of the effect of the antibiotic cargoes released from MSNs. In this regard, our research group has recently reported an interesting investigation to systematically and quantitatively evaluate the active doses released from different types of antibiotic-loaded MSNs [53]. In this sense, the biological active curves together with the impact of the active antibiotic cargo on Gram-positive (*Staphylococcus aureus*) and Gram-negative (*Escherichia coli*) bacterial biofilms. In Figure 6, a schematic depiction of the experimental design to carry out this type of study is shown. In such experiments, the doses of the different antibiotic cargoes released from MSNs "in vial", i.e., in an acellular physiological solution, as a function of time, are collected. Later, the released doses were quantified by using appropriate spectroscopic techniques; their biological activity and antibiofilm capacity was evaluated. Left graph in Figure 6 displays the active doses of levofloxacin, chosen as an illustrative example, at different times, against *S. aureus* bacteria (red curve). In addition, levofloxacin released doses during the in vial experiments are also shown (blue curve). Levofloxacin has a strong interaction with silica

surface at physiological pH through hydrogen bonds with silanol groups, being that this is association responsible for the in vial release behavior [53]. As it can be observed, both active and release doses patterns are similar, but the antibiotic released doses are ca. 10-fold higher than the active doses. This discrepancy is ascribed to a partial loosening of the antimicrobial activity of the antibiotic drug. Right graph in Figure 6 shows the results derived from the evaluation of the antibiofilm capacity in *S. aureus* bacteria. It has been shown that all the released doses significantly reduced the biofilm. This antibiofilm effect is maintained over time, reducing the biofilm above 99% during the first 48 h, and achieving a reduction of ca. 77% at 96 h. This is an essential study to demonstrate that MSNs are excellent nanocarriers to load and release antibiotics of diverse families, preserving their antimicrobial activity. Thus, MSNs constitute ideal nanoplatforms as starting point towards the design of advanced nanomedicines for the management of bone infection in future personalized therapies.

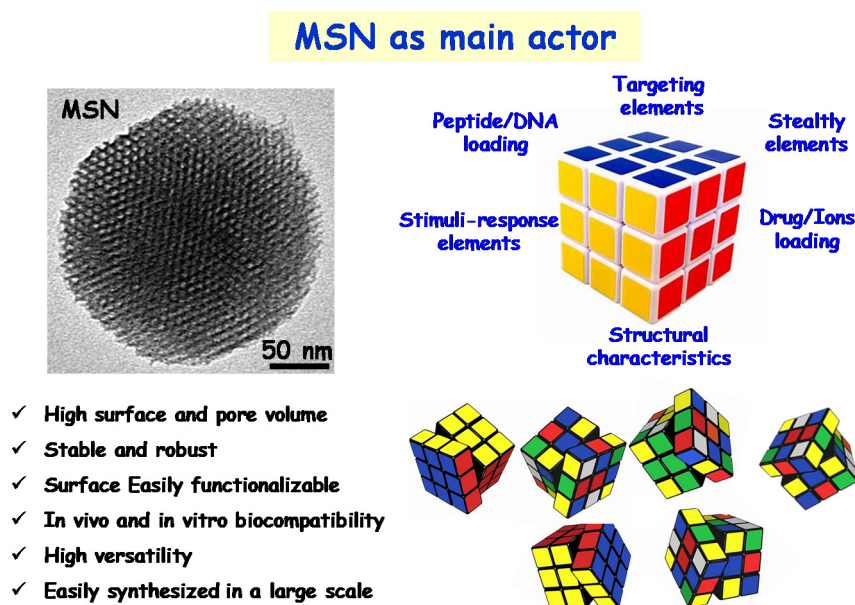


Figure 5. Role of MSN as one of the main actors in the design and development of a nanoantibiotic for infection treatment. Left: TEM image of a MSN and its main features as an ideal nanocarrier of antimicrobial agents. Right: illustrative simile between a MSN and a Rubik's cube to emphasize the different facets that can be adapted to design nanoantibiotics for future personalized therapies.

3.2. MSNs for Targeted Delivery of Antimicrobials

The use of targeted nanoparticles represents effective new alternatives for the management of bone infection facing the two major current problems associated with infectious diseases, antimicrobial bacterial resistance and biofilm formation. Hence, the design of MSNs as antimicrobial nanocarriers against bacterial infection implies targeting strategies that lead to an enhanced efficiency of antimicrobials due to the specific interaction of the MSNs with bacteria or biofilm. In this sense, decoration of the outermost surface of MSNs with targeting ligands that produce selective accumulation in the bacteria wall or the biofilm are the approaches of foremost relevance. By using these targeting strategies, the action of antimicrobials is combined with another mechanism due to the nanocarrier itself, such as destabilisation of the bacteria wall or promotion of biofilm penetrability, therefore enhancing their efficacy. The aim is to increase the selectivity and efficiency of antimicrobials, reducing doses and frequency of the administration, therefore preventing undesirable side effects associated with unspecific drug delivery.

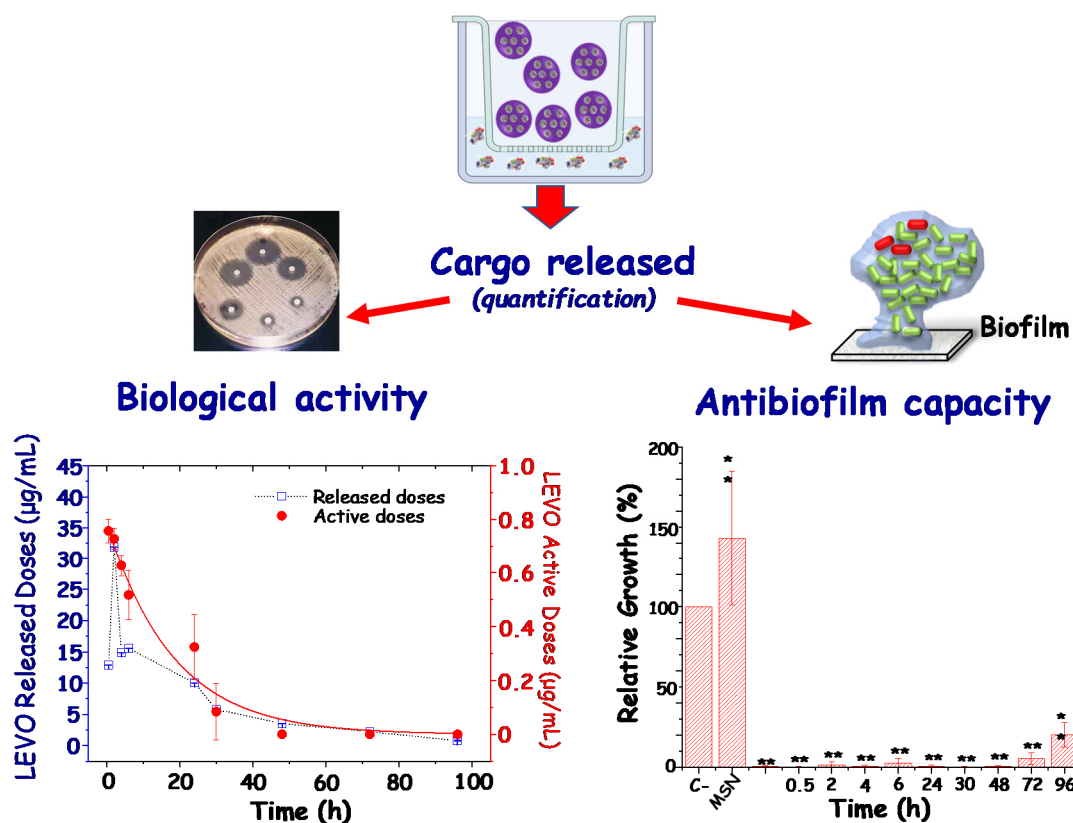


Figure 6. Top: Schematic depiction of the experimental design to carry out in vial drug delivery assays using antibiotic-loaded pure-silica MSNs, and subsequent quantification of cargo released doses, biological activity and antibiofilm capacity evaluations. Left graph: levofloxacin (LEVO) active doses against *S. aureus* bacteria (red curve) and LEVO released doses (blue curve) at different tested times. Right graph: In vitro antibiofilm activity of LEVO released doses in mature *S. aureus* biofilms. Adapted with permission from Aguilar et al. [53], *Micropor. Mesopor. Mat.*, published by Elsevier, 2021.

Just as MSNs have been successfully targeted as nanocarriers of anti-tumour drugs in the case of cancer [76,80], this concept also applies to bacterial infection. The wealth of knowledge and skills acquired in nanotechnology from basic research on smart MSN-based nanosystems for cancer therapy and diagnosis is facilitating the progress against infection by adapting to the particular characteristics of bacterial infection [29,38,40]. Active targeting provides nanosystems of specificity to the site of infection, being relevant in the case of intracellular infections, where bacteria overcome the host immune system by surviving in human cells. In this sense, MSNs have already been used as nanocarriers of anti-tuberculosis drugs [81,82], silver [83] or antimicrobial peptides [84] as antimycobacterial agents against intracellular *Mycobacterium tuberculosis*, the pathogen responsible for tuberculosis. This section describes recent advances in the pursuit of MSNs at the two main targets concerning infection management, the bacterium and the biofilm.

3.2.1. Targeting Bacteria

Bacteria targeting strategies involve floating or planktonic bacteria, i.e., isolated free-living bacteria. The presence of a cell wall is the main difference between bacterial and human cells. The bacterial cell wall is a protective layer mainly consisting of peptidoglycan and other glycolipids exclusive of bacteria, which plays an essential role in bacteria growth. These distinctive elements become excellent targets for planktonic bacteria. Therefore, it is feasible to discriminate between bacteria and human host cells, by attaching the appropriate targeting moiety in the surface of the nanosystems. In addition, it is also possible to distinguish between Gram-positive and Gram-negative bacteria, attending to the different structure of their bacterial cell wall.

Gram-positive bacteria possess a cytoplasmic membrane covered by a rigid and thick layer of peptidoglycans comprising carbohydrate polymers cross-linked through peptide residues [85]. On the other hand, Gram-negative bacteria possess a triple protective layer, involving a cytoplasmic membrane and a thinner, rigid peptidoglycan layer with shorter cross-links surrounded by a hydrophobic lipid bilayer consisting of lipopolysaccharides (LPS). This lipid layer presented on the surface forms a barrier that is responsible of the great resistance of Gram-negative bacteria to several antimicrobial agents [86].

Different approaches have exploited the “ligand-receptor binding” concept, searching for highly specific targeting nanosystems, using ligands that specifically bind surface molecules or receptors overexpressed in bacteria cell walls to decorate the outermost surface of MSNs. Some of the ligands include antibodies [87,88], aptamers [89], peptides [90,91], carbohydrates [92,93] and small molecules, such as amino acids [94], vitamins [95] and certain antibiotics [96].

In addition to targeting specific components of the bacterial membrane, different adsorption pathways for the nanoparticles can also be exploited [97]. For instance, Malmsten and co-workers have investigated the lipid membrane interactions of virus-like mesoporous nanoparticles, characterized by a biomimetic “spiky” external surface. The findings demonstrate that topography influences the interaction of nanoparticles with bacteria-mimicking lipid bilayers, as well as with bacteria, producing membrane binding and destabilization. These virus-like mesoporous nanoparticles that present spikes on the external surface have been tested as carriers for the antimicrobial peptide LL-37 against *E. coli* bacteria [98]. Following this approach, Ag nanocubes with biomimetic virus-like mesoporous silica coating loaded with gentamicin are capable of effectively adsorbing on the cell wall of both *E. coli* and *MRSA*. This core-shell nanostructure can be efficiently adsorbed on the rigid cell wall due to the virus-like surface, pulling through the low cell wall adhesion capability of typical antibacterial Ag nanoparticles [99].

A step forward in the design of MSNs with a biomimetic outer shell with a bacteria targeting capability was achieved by using outer membrane vesicles (OMVs) isolated from *E. coli* as coating. As bacterial vesicles preferentially enter the same type of bacteria, owing to their similar membrane structures, MSNs loaded with rifampicin and coated with these OMVs preferentially internalize by the same type of bacteria, resulting in an enhanced antibacterial efficacy [73].

Furthermore, electrostatic attractive interactions between negative charges in the outer bacterial membrane and positively charged nanoparticles can lead to the accumulation of the latter stacked to the bacteria wall, disturbing metabolic processes or causing perforation and even membrane leakage [100,101]. Several studies have evidenced that the presence of positive charges on the surface of NPs favours internalization in both Gram-positive and Gram-negative bacteria [102]. Hence, the use of antibiotic-loaded MSNs as nanovehicles with the ability to penetrate the bacterial wall is expected to increase the antimicrobial effectiveness.

For instance, polyamine functionalized MSNs prompt cell membrane disruption in Gram-positive *Listeria monocytogene*, increasing 100-fold their antimicrobial power compared to the free polyamines [103]. By using cationic polymers such as poly-L-lysine for capping MSNs, the enhancement of antimicrobials toxicity to Gram-negative bacteria is due to the bacterial wall damage induced by positively-charged lysine residues, which allows the entrapped cargo to gain access into the bacteria [104,105].

Examples of this kind of nanosystems developed in the Vallet-Regí's group comprise MSNs acting as nanocarriers of levofloxacin (LEVO) as antimicrobial agent localized inside the mesopores. These “nanoantibiotics” were externally functionalized with N-(2-aminoethyl)-3-aminopropyltrimethoxysilane [56] or a polycationic poly(propyleneimine) dendrimer of third generation (G3) as targeting agents [55]. The polyamine dendrimer was covalently grafted to the outer surface of LEVO-loaded MSNs and, after physicochemical characterization, the release kinetics of loaded LEVO and the antimicrobial efficacy of each released dosage were evaluated, displaying that the antibiotic was released in a sustained

fashion at effective bactericidal dosages. Moreover, internalization studies of the MSNs decorated with polycationic G3 dendrimer in *E. coli* bacteria showed a high penetrability throughout the Gram-negative bacterial membranes (see Figure 7). The high density of positive charges and flexibility on the surface of G3-MSNs produce attractive electrostatic interactions with the negatively charged bacterial walls, which triggers membrane permeabilization, and thus favours the nanosystem internalization. These studies also demonstrate that the combination of the cell wall disruption capability of G3 dendrimer and the bactericide effect of LEVO into a unique MSNs-based nanosystem has a synergistic antimicrobial effect on Gram-negative bacterial biofilm.

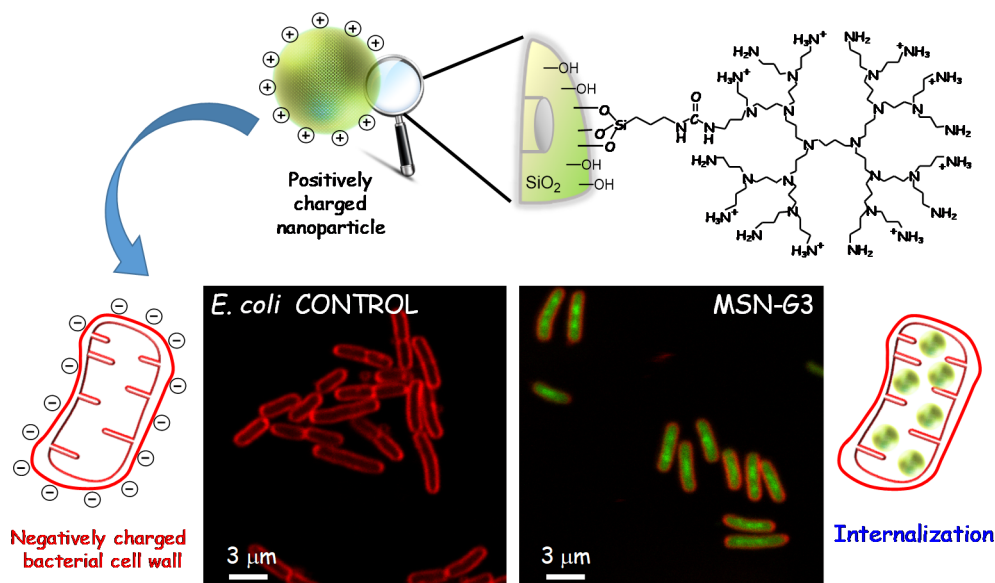


Figure 7. Schematic illustration showing MSNs nanosystem externally decorated with the poly(propyleneimine) dendrimer of third generation (G3) via covalent functionalization and its interaction with Gram-negative *E. coli* bacteria. The attractive forces between positive charges of the dendrimer on the surface of MSNs and negative charges on bacterial cell wall prompt cell membrane disruption and internalization of the nanosystem. Confocal microscopy images show *E. coli* control culture (left) and bacteria after exposure to 10 $\mu\text{g}/\text{mL}$ of the MSN-G3 nanosystem during an incubation time of 90 min (right). The *E. coli* cell membrane was stained in red and the MSN materials have previously been fluorescently tagged in green. Adapted with permission from González et al. [55], *Acta Biomater.*, published by Elsevier, 2018.

3.2.2. Targeting Biofilm

Another challenge that society faces against bacterial infection is the ability of bacteria to form biofilms, which hinders any conventional treatment for chronic infections and has serious socio-economic implications.

Biofilms are complex bacterial communities embedded in a protective exopolysaccharide (EPS) matrix. This self-produced matrix is composed of extracellular DNA, polysaccharides, proteins, glycolipids and other ionic molecules [9]. The EPS matrix protects the bacteria from hostile environmental conditions and reduces the efficacy of antibiotics by up to 100-fold compared to planktonic cells [106]. The formation of biofilms is a multistep process in which planktonic bacteria firstly adhere to a surface. Subsequently, the bacteria multiply to form microcolonies which develop into well-defined three-dimensional structures and which eventually produce the EPS coating around them. At times, the biofilm matrix breaks and free bacteria disperse, leading to a spread in infection [107].

Therefore, the nanotechnological approaches are different when working with bacteria associated in communities forming biofilms instead of the same kind of bacteria in planktonic state. Targeting bacterial biofilms with nanocarriers capable of overcoming the

barrier of the mucopolysaccharide matrix of the biofilm and releasing its loaded-antibiotic within this matrix would be highly desirable. The emerging research field regarding MSNs able to disrupt the EPS, penetrate bacterial biofilm and release the antimicrobial cargo, constitutes a promising alternative to eradicate bacterial biofilms.

Recent approaches focus on MSNs for the delivery of antibiofilm agents such as certain enzymes able to reduce EPS cohesiveness and disperse the biofilm biomass, for example lysozyme [108] or DNase I [109]. Moreover, taking into account that the EPS components typically exhibit negative charges, the nanoparticle-biofilm interactions can be increased by tailoring the surface charge of the MSNs. For instance, positively charged vancomycin-loaded MSNs were more efficiently localized to the surface of biofilm cells and were more active in reducing biofilm cell viability than MSNs having more vancomycin loaded but negatively charged [110].

In this sense, professor Vallet-Regí's group reported the design of antibiotic nanocarriers able to penetrate bacterial biofilm using positively charged moieties as the targeting agents on the external surface of the MSNs. Amine functionalization of the MSNs with N-(2-aminoethyl)-3-aminopropyltrimethoxy-silane provides positive charges, improving the affinity of the LEVO loaded nanosystem towards the negatively charged bacteria wall and biofilm. Physicochemical characterization of the nanosystem, in vial LEVO release profiles and the in vitro antimicrobial effectiveness of the different released doses were investigated. The efficacy of this nanoantibiotic was evaluated against a *S. aureus* biofilm, showing its near-total destruction due to the high penetration ability of the developed nanosystem. Biofilm eradication is achieved thanks to the synergistic combination of antibiotic and targeting agent in a unique nanoplatform [56]. High anti-biofilm efficiency against Gram-negative *E. coli* bacteria was also accomplished throughout the synergistic action of polycationic dendrimers (G3), as bacterial membrane permeabilization agents, and LEVO loaded in the mesopores of MSNs as well [55].

An alternative biofilm-targeting strategy, consisting of decorating the outer surface of MSNs with molecules possessing affinity towards certain components present in the EPS, has been described by the same research group. The lectin concanavalin A (ConA) is a protein able to recognize and bind to glycan-type polysaccharides present in the biofilm EPS and, owing to this affinity, was chosen as the targeting ligand. This new nanosystem was obtained by functionalizing MSNs with carboxylic acid groups, covalently attaching ConA and loading LEVO in the mesopores. The bacterial biofilm-targeting efficacy of the nanocarrier was evaluated in *E. coli* biofilms showing that the presence of ConA in the external surface of the nanosystem promotes its internalization into the biofilm matrix in a dose dependent internalization fashion. The release of the mesopore hosted LEVO inside the biofilm is made possible thanks to the ConA-driven penetration of the nanosystem into the matrix, thus increasing the antimicrobial efficacy of the antibiotic. Hence, the synergistic combination of ConA and LEVO in the same nanoplatform lead to a complete biofilm destruction (see Figure 8) [111].

A similar approach for biofilm targeting makes use of Arabic gum as a coating of MSNs. This branched-chain complex polysaccharide is composed of 1,3-linked beta-D-galactopyranosyl monomers connected to the main chain through 1,6-linkages, whose degradation by secreted bacterial enzymes improves the retention of MSNs on the biofilm. The nanosystem demonstrated high affinity toward *E. coli* biofilm matrix, thanks to the Arabic gum coating and, loaded with two clinically relevant antibiotics such as moxifloxacin and colistin, exhibits substantial in vivo efficacy against an osteomyelitis provoked by *E. coli* [112].

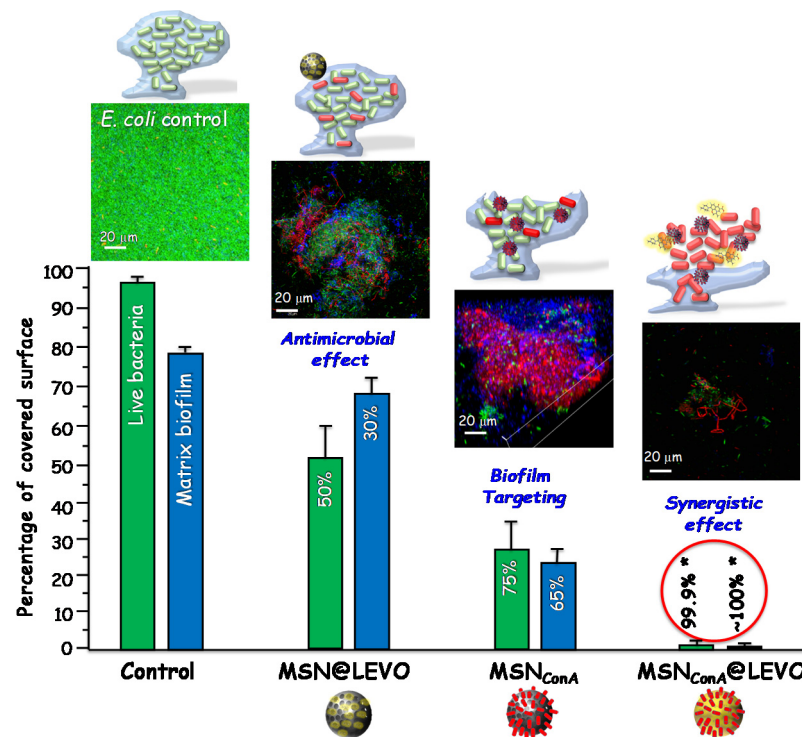


Figure 8. Antimicrobial activity of levofloxacin loaded and Concanavalin A functionalized MSNs against *E. coli* biofilm. The histogram represents the reduction in percentage of covered surface of live bacteria (green bars) and mucopolysaccharide matrix (blue bars), calculated from the confocal microscopy images (top). The images were obtained after exposure of a preformed biofilm to the different nanosystems during 90 min of incubation. Live bacteria are stained in green, dead bacteria in red, and the protective matrix biofilm in blue. A synergistic effect is achieved when the MSNs are loaded with levofloxacin and functionalized with ConA which acts as targeting agent for the mucopolysaccharide matrix and allows the release of the antibiotics inside the biofilm. Adapted with permission from Martínez-Carmona et al. [111], *Acta Biomater.*, published by Elsevier, 2019.

3.3. Combined Therapies

Once the ability of these MSNs to internalise into the bacteria and the biofilm has been demonstrated, the second challenge in the fight against antimicrobial resistance consists in the design of nanosystems with enhanced antimicrobial efficacy, through the combination of different antimicrobial elements within the same nanoplatform. To this aim, different research groups have reported innovative strategies based in either the co-delivery of antibiotics [112–115], or the combination of antibiotics plus antimicrobial metal nanoparticles or ions [28].

Regarding the first approach, the most straightforward and easiest way is to simultaneously co-load different antibiotic molecules into the pores of MSNs. Thus, Gurnani et al. [113] co-loaded polymyxin B and vancomycin into MSNs with high efficiency, showing high bactericidal effect against Gram-negative and Gram-positive bacteria. However, the co-encapsulation of drugs with different and occasionally opposite physicochemical properties within a single MSN-based nanocarrier requires developing compartmentalization strategies. Along this line, Meber et al. [114] reported the synthesis of core-shell MSNs to simultaneously deliver gentamicin and rifamycin by using a multilayer construction of MSNs, following a step-by-step loading of these antibiotics. In a very recent study, Aguilera-Correa et al. [112] described an original methodology to engineer moxifloxacin-loaded MSNs coated with Arabic gum plus colistin to address *E. coli* bone infections. Significant antibacterial in vitro and in vivo efficacy was observed thanks to the Arabic gum targeting capability towards *E. coli* biofilm, the disaggregating and

antibacterial effect of colistin, and a remarkable antibiofilm action due to the bactericidal activity of moxifloxacin and colistin. Another interesting methodology to co-deliver therapeutic agents of different chemical nature relies on using asymmetric MSNs with anisotropic geometry and two compartments able to load drugs of different nature in separated storage spaces. Within this context, Cheng et al. [115] reported innovative core-shell magnetic MSNs grafted to ethane-bridged mesoporous periodic organosilica with different loading properties. Gentamicin and curcumin were independently loaded into the hydrophilic and hydrophobic spaces, to provide the nanosystem of dual antibacterial and antitumor capability.

Concerning the second approach, in recent decades certain antimicrobial agents, such as some metals, metal oxides and metal salts are re-emerging in the treatment of infected prostheses. Such metals have been known for centuries for their intrinsic antibacterial properties and were used to treat bacterial and fungal infections before the discovery of penicillin by Sir Alexander Fleming. Although their medicinal utility declined with the antibiotic era, the emergence of antibiotic resistance has led to their recovery as antimicrobials. In fact, the use of some metals against bacterial infection is currently growing exponentially due to improved synthesis routes that allow the production of less toxic nanoparticles or metal oxides materials [116]. Among metal and metal oxide nanoparticles, silver nanoparticles are probably the most promising of all the inorganic nanoparticles as a treatment for bacterial infections [20]. Besides Ag, other metal nanoparticles such as Au, and metal oxide nanoparticles, such as ZnO, CuO, iron oxides (γ -Fe₂O₃, Fe₃O₄), and TiO₂, among others, are being intensively studied for antimicrobial treatment [18,117].

However, despite the bactericidal potential of metal nanoparticles and metal ions, their use in biomedical applications is limited due to their high toxicity [118–120]. Therefore, a selective administration by carrying them in another vehicle would prevent systemic exposure to metallic species as well as the aggregation problems associated to uncoated metallic nanoparticles [121]. In this context, the use of MSNs as nanocarriers of silver nanoparticles has been reported for cancer [80,122] and infection treatments [83,123–127].

In a pioneering research project, Wang et al. [123] reported innovative core-shell nanosystems consisting in Ag nanoparticles as cores and levofloxacin-loaded MSNs as shells. This study proved that the Ag core dissolved slowly, releasing Ag⁺, which in combination with the antibiotic release, produced a synergistic antibacterial effect against drug-resistant infections both in vitro and in vivo. Very recently, and taking into account the advances achieved by María Vallet-Regí's research group in the targeting of antibiotic-loaded nanosystems towards bacteria or biofilm using MSNs externally decorated with polyamine dendrimers (Section 3.2) [55], a totally different and groundbreaking idea was conceived, that is, using MSN-G3 nanoplatfoms as vehicles for metal cations with antimicrobial properties. A great advantage of this nanoplatfom is the high content in amine groups due to the dendrimer that allows for the complexation of multiactive metal cations through coordination bonds.

Therefore, a simple and versatile methodology has been recently reported by using MSNs externally decorated with G3 dendrimers for the complexation of antimicrobial metal ions (Mⁿ⁺) by soaking the MSN-G3 nanosystem into a M(NO₃)_n aqueous solution [128]. This methodology allows incorporating a wide range of both antibiotics and metal ions, which permits adapting the antimicrobial cargoes to the patient clinical requirements. The selection of the cation may be done depending on clinical needs. Thus, the treatment of different pathogenic bacterial biofilms can be tailored by simply changing the loaded antibiotic attending to the clinical needs. In such work, levofloxacin, a broad spectrum antibiotic, and Zn²⁺ ion, with dual antimicrobial and osteogenic capabilities, were selected. These multicomponent nanosystems exhibited an excellent in vitro biocompatibility in MC3T3-E1 preosteoblasts cultures, and remarkable antimicrobial effect above 99% compared to the MSNs that only contained one of the antimicrobial elements. In addition, the incorporation of Zn²⁺ in the whole nanosystem promoted bone repair associated to osteolysis by stimulating bone cell differentiation. In this sense, this innovative nanosystems opens up a new

scientific paradigm since the presence of metal ions may aid to prevent the emergence of antibiotic resistances, while reducing toxicity risks.

3.4. Stimuli-Responsive

The ideal drug nanocarrier required to fight infection must both protect the antimicrobial cargo and be able to successfully transport it to the desired cell or tissue [2,28,29,38,39,129]. When it reaches its destination, the nanocarrier must release the drug(s) in a controlled manner and in the desired concentrations. In this sense, MSNs are the perfect nanomaterial to carry out a combined therapy, since they can host in their mesopores different drugs or combinations of antibiotics that can act synergistically in the focus of the infection [2,28,29,38,39,53,77,111,128].

In order to successfully perform this function, there are several strategies to place on the pore outlets' different organic or inorganic moieties acting as pore blockers or gatekeepers, preventing premature release of cargo [2,27,28,130–132]. These strategies respond to the application of various stimuli that trigger the release of the antimicrobial load at the site of infection [28,39,111]. These smart nanosystems can carry the drug content to the target cell or tissue. Once there, the presence of internal or external stimulus will trigger the drugs release in a control manner [2,28,29,32,55,111,133–136].

In the case of external stimuli an external apparatus is frequently required to trigger the release, while in the case of internal stimuli applied to nanocarriers based on MSNs no external apparatus is required [28,29,32,39,137]. However, the control over the administered dose is less than in the case of devices that use an external stimulus. In order to choose which system to use successfully, it is necessary to consider that the exact clinical application to be solved must be taken into account and the system adapted to it. Among the internal-responsive stimuli, the most used are the presence of bacteria [104], bacterial toxins [138], redox potential [139], pH [29]. Among the external-responsive stimuli, the most important are those related to chemical species [140], light [141–143] temperature [29] or the alternating magnetic field [29]. In addition, it is possible to combine two or more internal or external stimuli to improve the therapeutic effect of the MSN nanocarriers [2,29,144,145].

For example, among the internal-responsive stimuli, one can take advantage of the decrease in pH values that has been observed in infections, after surgery or loosening of an implant [2,29,146–148] to create pH stimuli-responsive nanocarriers based on MSN for detection and eradication of bacteria that only release their contents when the pH is low [2,29,149]. In these situations, the pH usually decreases from pH 7.35–7.45 in non-infected tissues to pH < 7 in bone infection and trigger some variations in the surface charge of biomaterials, in the isoelectric point and bacterial adhesion capacity, increasing the infections. Among the external-responsive stimuli, it is possible to design nanosystems based on MSN loaded with antimicrobial drugs and coated with different redox-sensitive molecules, as disulfide snap-tops [139]. This disulfide bond, and other types, can be cleaved in reducing environments and the antibiotic release is produced intracellularly, inhibiting the presence of bacteria [29].

Professor María Vallet-Regí's research group has widespread experience in stimulus-response nanosystems based on MSNs in the treatment of several types of cancer cells, with numerous studies associated with the application of different internal and external stimuli in this area [25,28,30]. Specifically, this group has developed studies with nanosystems based on MSNs related to internal stimulus-response such as pH [150–153] or redox processes [154], and the application of several external stimuli as ultrasounds [155–158], magnetic field [159,160], photothermal therapy [161] or visible light [162]. In addition, the combination of therapeutic approaches has been proven as a complementary approach for conventional chemotherapy. In this sense, Vallet-Regí's research group has developed nanocarriers that combined several of these internal or external stimuli [155,163,164].

The previous experience of the group in these types of stimuli-response nanosystems in the field of cancer has facilitated the possibility of developing the recent published study of María Vallet-Regí's group, focused on the successful inhibition of biofilm through

photothermal therapy with Near Infra-Red (NIR) light by gold core@shell based MSNs loaded with levofloxacin (LEVO) and nitric oxide (NO) (Figure 9) [165].

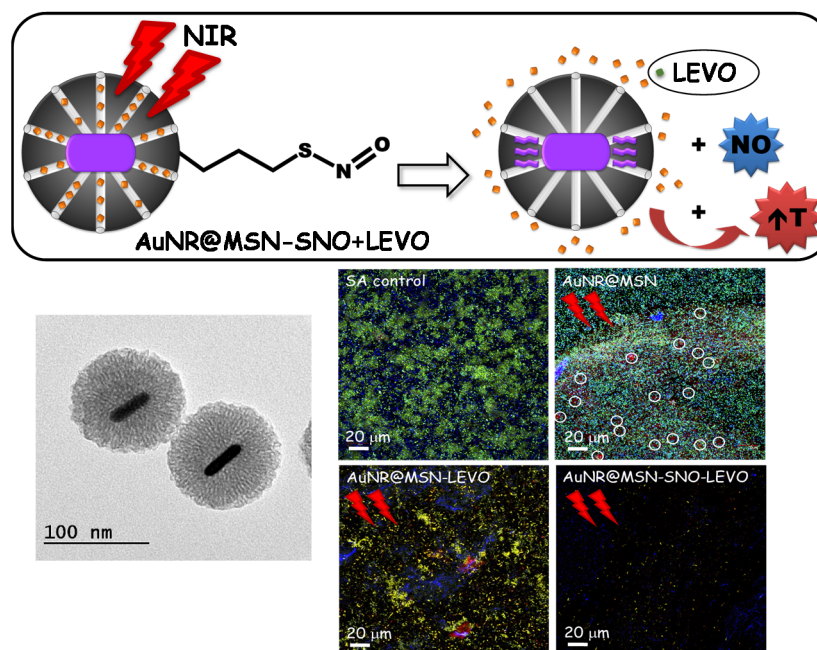


Figure 9. Top image: schematic representation of the nanocarrier design AuNR@MSN-SNO+LEVO and its effect on a *S. aureus* biofilm in response to near infra-red (NIR) laser treatment. Bottom left image: transmission electron microscopy micrographs of AuNRs surrounded by a mesoporous silica shell of AuNR@MSN-PEG_{ext} nanocarriers. Bottom right: confocal microscopy images of the antimicrobial action of AuNR@MSN nanocarriers onto Gram-positive *S. aureus* (SA) biofilm. These images depict the biofilm performed without treatment (SA CONTROL), and after incubation with AuNR@MSN, AuNR@MSN+LEVO and AuNR@MSN-SNO+LEVO nanocarriers with subsequent NIR treatment. Live bacteria are stained in green, dead bacteria in red, ablation zones are marked with white circles, and the extracellular polysaccharide matrix biofilm is stained in blue. Adapted with permission from García et al. [165], Micropor. Mesopor. Mat., published by Elsevier, 2021.

As discussed previously, bacterial biofilms can trigger chronic infections that are difficult to resolve; there are still no satisfactory alternatives to prevent and cure them [149]. In this context, different approaches for biofilm disruption were designed to destroy the protective layer and remove biofilm bacteria (DNase, proteases, cationic molecules, light-activated antimicrobial agents) [166–168]. María Vallet-Regí's group has designed light-sensitive MSNs with combined photothermal (PTT) and antimicrobial properties [165]. PTT therapy has exposed a bactericidal mechanism, mostly efficient in the near NIR spectral range (650–900 nm), based on the conversion of light into localized heating and robust absorption of nanomaterials [143,169].

The development of nanosystems such as the one proposed offers a new strategy with higher efficacy, increasing the local concentration of the drug in the biofilm, and lower side actions, as it is a localized effect without causing serious injury to healthy tissues [2,29,38,53,77]. These nanocarriers acquire a great impact in the infection clinical field as they can affect the architecture of the *Staphylococcus aureus* bacterial biofilm, decreasing its growth.

On the one hand, this nanocarrier possesses photothermal therapy due to the incorporation of gold nanorods followed by the growth of a silica shell leads to a core@shell-type design (AuNR@MSN) with PTT properties. On the other hand, the LEVO is loaded into the nanocarriers' mesoporous channels, while the nitric oxide (NO) is bonded through nitrothiol groups (-SNO), a heat-labile linker, consequently allowing a higher NO delivery

through the increase of temperature upon NIR activation [165]. Release of exogenous NO has revealed potential clinical applications in several diseases, such as cancer, cardiovascular disorders and bacterial infections [165]. Regarding infection, NO has been shown to be a crucial regulator of biofilm dispersion [170], and to trigger antibacterial action through the generation of by-products that affect oxidative and nitrosative stress [170]. In addition, it has also demonstrated its effect against biofilm dispersion when combined with conventional antibiotics [171]. The combination of these factors under a stimulus-response nanosystem produces a unique nanoassembly with potential therapeutic efficacy against *S. aureus* biofilms as can be deduced from the results obtained in this study [165]. The authors first describe the synthesis and physicochemical characterization of the nanocarriers to perform an in vitro LEVO release study with or without NIR activation and the optimization of the parameters for *S. aureus* bacterial biofilm destruction. For this purpose, preformed *S. aureus* biofilms were cultured with the different nanocarriers at a final concentration of 50 µg/mL for 90 min before first NIR laser application (808 nm, 1 W/cm², 10 min). The same process was repeated after another 90 min of incubation and then all samples were incubated for 24 h at 37 °C. When light stimuli were applied, a 30% decrease of the *S. aureus* biofilm was observed with the antibiotic LEVO and its illumination with NIR irradiation displayed a biofilm reduction of 90% (Figure 9). These results denote that the combination of specific antimicrobial drug release (levofloxacin and nitric oxide) at the site of infection and PTT upon NIR irradiation disrupt the integrity of bacterial biofilms, improving the therapeutic efficiency of alternative treatments [165]. At present, Professor Vallet-Regí's research group continues to explore more stimulus-response nanosystems to fight infection.

4. Conclusions

The discovery of antibiotics was one of the major breakthroughs for humanity in the management of bacterial infections. Nonetheless, nowadays we are facing a new post-antibiotic era since bacteria have developed defense mechanisms that make them highly resistant to the existing antibiotics. This challenging issue has motivated the scientific community to develop new alternative treatments to fight infection. Nanotechnology has entered this scenario providing nanomaterials as nanocarriers of different antimicrobial agents, denoted as nanoantibiotics. Among nanocarriers, mesoporous silica nanoparticles own superlative properties and constitute ideal nanoplatforms to design targeted and stimuli-response release systems of different antimicrobial agents. These multifunctional nanosystems are foreseen as advanced antimicrobial nanoformulations for clinical application in customized therapies.

Author Contributions: All authors have been involved in the conceptualization, writing—original draft and writing—review and editing. All authors have read and agreed to the published version of the manuscript.

Funding: This research was funded by European Research Council, Advanced Grant VERDI, ERC-2015-AdG proposal no. 694160 and the Ministerio de Ciencia e Innovación (PID2020-117091RB-I00 grant).

Institutional Review Board Statement: Not applicable.

Informed Consent Statement: Not applicable.

Data Availability Statement: Not applicable.

Acknowledgments: The authors would like to express their sincere and deepest thanks to María Vallet-Regí for her tireless dedication to the science that has been the source of inspiration for our careers, as well as for the opportunity to work alongside her. Gracias Marita.

Conflicts of Interest: The authors declare no conflict of interest.

References

1. Maradit Kremers, H.; Larson, D.R.; Crowson, C.S.; Kremers, W.K.; Washington, R.E.; Steiner, C.A.; Jiranek, W.A.; Berry, D.J. Prevalence of Total Hip and Knee Replacement in the United States. *J. Bone Joint Surg. Am.* **2015**, *97*, 1386–1397. [CrossRef] [PubMed]
2. Vallet-Regí, M.; Lozano, D.; González, B.; Izquierdo-Barba, I. Biomaterials against Bone Infection. *Adv. Healthcare Mater.* **2020**, *9*, 2000310. [CrossRef] [PubMed]
3. WHO. New Report Calls for Urgent Action to Avert Antimicrobial Resistance Crisis. Available online: <https://www.who.int/news/item/29-04-2019-new-report-calls-for-urgent-action-to-avert-antimicrobial-resistance-crisis> (accessed on 15 November 2021).
4. Saeed, K.; McLaren, A.C.; Schwarz, E.M.; Antoci, V.; Arnold, W.V.; Chen, A.F.; Clauss, M.; Esteban, J.; Gant, V.; Hendershot, E.; et al. 2018 international consensus meeting on musculoskeletal infection: Summary from the biofilm workgroup and consensus on biofilm related musculoskeletal infections. *J. Orthop. Res.* **2019**, *37*, 1007–1017. [CrossRef] [PubMed]
5. Schwarz, E.M.; Parvizi, J.; Gehrke, T.; Aiyer, A.; Battenberg, A.; Brown, S.A.; Callaghan, J.J.; Citak, M.; Egol, K.; Garrigues, G.E.; et al. 2018 International Consensus Meeting on Musculoskeletal Infection: Research Priorities from the General Assembly Questions. *J. Orthop. Res.* **2019**, *37*, 997–1006. [CrossRef] [PubMed]
6. Rosas, S.; Ong, A.C.; Buller, L.T.; Sabeh, K.G.; Law, T.Y.; Roche, M.W.; Hernandez, V.H. Season of the year influences infection rates following total hip arthroplasty. *World J. Orthop.* **2017**, *8*, 895–901. [CrossRef] [PubMed]
7. Kaplan, S.L. Recent lessons for the management of bone and joint infections. *J. Infect.* **2014**, *68* (Suppl. 1), S51–S56. [CrossRef] [PubMed]
8. Hall-Stoodley, L.; Costerton, J.W.; Stoodley, P. Bacterial biofilms: From the natural environment to infectious diseases. *Nat. Rev. Microbiol.* **2004**, *2*, 95–108. [CrossRef]
9. Davies, D. Understanding biofilm resistance to antibacterial agents. *Nat. Rev. Drug Discov.* **2003**, *2*, 114–122. [CrossRef]
10. Kumar, A.; Alam, A.; Rani, M.; Ehtesham, N.Z.; Hasnain, S.E. Biofilms: Survival and defense strategy for pathogens. *Int. J. Med. Microbiol.* **2017**, *307*, 481–489. [CrossRef]
11. Høiby, N.; Bjarnsholt, T.; Givskov, M.; Molin, S.; Ciofu, O. Antibiotic resistance of bacterial biofilms. *Int. J. Antimicrob. Agents* **2010**, *35*, 322–332. [CrossRef]
12. Masters, E.A.; Trombetta, R.P.; de Mesy Bentley, K.L.; Boyce, B.F.; Gill, A.L.; Gill, S.R.; Nishitani, K.; Ishikawa, M.; Morita, Y.; Ito, H.; et al. Evolving concepts in bone infection: Redefining “biofilm”, “acute vs. chronic osteomyelitis”, “the immune proteome” and “local antibiotic therapy”. *Bone Res.* **2019**, *7*, 20. [CrossRef]
13. Redlich, K.; Smolen, J.S. Inflammatory bone loss: Pathogenesis and therapeutic intervention. *Nat. Rev. Drug Discov.* **2012**, *11*, 234–250. [CrossRef]
14. Putnam, N.E.; Fulbright, L.E.; Curry, J.M.; Ford, C.A.; Petronglo, J.R.; Hendrix, A.S.; Cassat, J.E. MyD88 and IL-1R signaling drive antibacterial immunity and osteoclast-driven bone loss during *Staphylococcus aureus* osteomyelitis. *PLoS Pathog.* **2019**, *15*, e1007744. [CrossRef]
15. Arciola, C.R.; Campoccia, D.; Montanaro, L. Implant infections: Adhesion, biofilm formation and immune evasion. *Nat. Rev. Microbiol.* **2018**, *16*, 397–409. [CrossRef]
16. O’Neill, J. Antimicrobial Resistance: Tackling a crisis for the health and wealth of nations. *Rev. Antimicrob. Resist.* **2014**, *1*, 1–16.
17. Campoccia, D.; Montanaro, L.; Arciola, C.R. A review of the biomaterials technologies for infection-resistant surfaces. *Biomaterials* **2013**, *34*, 8533–8554. [CrossRef]
18. Gold, K.; Slay, B.; Knackstedt, M.; Gaharwar, A.K. Antimicrobial Activity of Metal and Metal-Oxide Based Nanoparticles. *Adv. Ther.* **2018**, *1*, 1700033. [CrossRef]
19. Garino, N.; Sanvitale, P.; Dumontel, B.; Laurenti, M.; Colilla, M.; Izquierdo-Barba, I.; Cauda, V.; Vallet-Regí, M. Zinc oxide nanocrystals as a nanoantibiotic and osteoinductive agent. *RSC Adv.* **2019**, *9*, 11312–11321. [CrossRef]
20. Burduşel, A.-C.; Gherasim, O.; Grumezescu, A.M.; Mogoantă, L.; Ficai, A.; Andronescu, E. Biomedical Applications of Silver Nanoparticles: An Up-to-Date Overview. *Nanomaterials* **2018**, *8*, 681. [CrossRef]
21. Huh, A.J.; Kwon, Y.J. “Nanoantibiotics”: A new paradigm for treating infectious diseases using nanomaterials in the antibiotics resistant era. *J. Control. Release* **2011**, *156*, 128–145. [CrossRef]
22. Mamun, M.M.; Sorinolu, A.J.; Munir, M.; Vejerano, E.P. Nanoantibiotics: Functions and Properties at the Nanoscale to Combat Antibiotic Resistance. *Front. Chem.* **2021**, *9*, 687660. [CrossRef]
23. Vallet-Regí, M. Our Contributions to Applications of Mesoporous Silica Nanoparticles. *Acta Biomater.* **2021**. [CrossRef]
24. Baeza, A.; Colilla, M.; Vallet-Regí, M. Advances in mesoporous silica nanoparticles for targeted stimuli-responsive drug delivery. *Expert Opin. Drug Deliv.* **2015**, *12*, 319–337. [CrossRef]
25. Baeza, A.; Manzano, M.; Colilla, M.; Vallet-Regí, M. Recent advances in mesoporous silica nanoparticles for antitumor therapy: Our contribution. *Biomater. Sci.* **2016**, *4*, 803–813. [CrossRef]
26. Carvalho, G.C.; Sábio, R.M.; de Cássia Ribeiro, T.; Monteiro, A.S.; Pereira, D.V.; Ribeiro, S.J.L.; Chorilli, M. Highlights in Mesoporous Silica Nanoparticles as a Multifunctional Controlled Drug Delivery Nanoplatfor for Infectious Diseases Treatment. *Pharm. Res.* **2020**, *37*, 191. [CrossRef]
27. Castillo, R.R.; Lozano, D.; Vallet-Regí, M. Mesoporous Silica Nanoparticles as Carriers for Therapeutic Biomolecules. *Pharmaceutics* **2020**, *12*, 432. [CrossRef]

28. Castillo, R.R.; Vallet-Regí, M. Recent Advances Toward the Use of Mesoporous Silica Nanoparticles for the Treatment of Bacterial Infections. *Int. J. Nanomed.* **2021**, *16*, 4409–4430. [CrossRef]
29. Colilla, M.; Vallet-Regí, M. Targeted Stimuli-Responsive Mesoporous Silica Nanoparticles for Bacterial Infection Treatment. *Int. J. Mol. Sci.* **2020**, *21*, 8605. [CrossRef] [PubMed]
30. Gisbert-Garzarán, M.; Manzano, M.; Vallet-Regí, M. Mesoporous Silica Nanoparticles for the Treatment of Complex Bone Diseases: Bone Cancer, Bone Infection and Osteoporosis. *Pharmaceutics* **2020**, *12*, 83. [CrossRef] [PubMed]
31. Manzano, M.; Vallet-Regí, M. New developments in ordered mesoporous materials for drug delivery. *J. Mater. Chem.* **2010**, *20*, 5593–5604. [CrossRef]
32. Vallet-Regí, M.; Colilla, M.; Izquierdo-Barba, I.; Manzano, M. Mesoporous Silica Nanoparticles for Drug Delivery: Current Insights. *Molecules* **2018**, *23*, 47. [CrossRef]
33. Sábio, R.M.; Meneguín, A.B.; Martins dos Santos, A.; Monteiro, A.S.; Chorilli, M. Exploiting mesoporous silica nanoparticles as versatile drug carriers for several routes of administration. *Microporous Mesoporous Mater.* **2021**, *312*, 110774. [CrossRef]
34. Valetti, S.; Thomsen, H.; Wankar, J.; Falkman, P.; Manet, I.; Feiler, A.; Ericson, M.B.; Engblom, J. Can mesoporous nanoparticles promote bioavailability of topical pharmaceuticals? *Int. J. Pharm.* **2021**, *602*, 120609. [CrossRef]
35. García-Fernández, A.; Sancenón, F.; Martínez-Mañez, R. Mesoporous silica nanoparticles for pulmonary drug delivery. *Adv. Drug Deliv. Rev.* **2021**, *177*, 113953. [CrossRef]
36. Vallet-Regí, M. Infection. Available online: <https://www.youtube.com/watch?v=kssRgcEfiW4> (accessed on 15 November 2021).
37. Vallet-Regí, M.; Rámila, A.; del Real, R.P.; Pérez-Pariente, J. A New Property of MCM-41: Drug Delivery System. *Chem. Mater.* **2001**, *13*, 308–311. [CrossRef]
38. Vallet-Regí, M.; González, B.; Izquierdo-Barba, I. Nanomaterials as Promising Alternative in the Infection Treatment. *Int. J. Mol. Sci.* **2019**, *20*. [CrossRef]
39. Martínez-Carmona, M.; Gun'ko, Y.K.; Vallet-Regí, M. Mesoporous Silica Materials as Drug Delivery: “The Nightmare” of Bacterial Infection. *Pharmaceutics* **2018**, *10*, 279. [CrossRef]
40. Bernardos, A.; Piacenza, E.; Sancenón, F.; Hamidi, M.; Maleki, A.; Turner, R.J.; Martínez-Mañez, R. Mesoporous Silica-Based Materials with Bactericidal Properties. *Small* **2019**, *15*, 1900669. [CrossRef]
41. Selvarajan, V.; Obuobi, S.; Ee, P.L.R. Silica Nanoparticles-A Versatile Tool for the Treatment of Bacterial Infections. *Front. Chem.* **2020**, *8*, 602. [CrossRef]
42. Vallet-Regí, M.; Colilla, M.; González, B. Medical applications of organic-inorganic hybrid materials within the field of silica-based bioceramics. *Chem. Soc. Rev.* **2011**, *40*, 596–607. [CrossRef]
43. Vallet-Regí, M.; Balas, F.; Arcos, D. Mesoporous Materials for Drug Delivery. *Angew. Chem. Int. Ed.* **2007**, *46*, 7548–7558. [CrossRef]
44. Vallet-Regí, M.; Izquierdo-Barba, I.; Colilla, M. Structure and functionalization of mesoporous bioceramics for bone tissue regeneration and local drug delivery. *Philos. Trans. A Math. Phys. Eng. Sci.* **2012**, *370*, 1400–1421. [CrossRef]
45. Zhuravlev, L.T. Concentration of hydroxyl groups on the surface of amorphous silicas. *Langmuir* **1987**, *3*, 316–318. [CrossRef]
46. Zhuravlev, L.T. The Surface Chemistry of Amorphous Silica. Zhuravlev Model. *Colloids Surf. A* **2000**, *173*, 1–38. [CrossRef]
47. Vallet-Regí, M. Ordered Mesoporous Materials in the Context of Drug Delivery Systems and Bone Tissue Engineering. *Chem. Eur. J.* **2006**, *12*, 5934–5943. [CrossRef]
48. Hoffmann, F.; Cornelius, M.; Morell, J.; Fröba, M. Silica-Based Mesoporous Organic-Inorganic Hybrid Materials. *Angew. Chem. Int. Ed.* **2006**, *45*, 3216–3251. [CrossRef]
49. Yang, P.; Gaib, S.; Lin, J. Functionalized mesoporous silica materials for controlled drug delivery. *Chem. Soc. Rev.* **2012**, *41*, 3679–3698. [CrossRef] [PubMed]
50. Huang, R.; Shen, Y.-W.; Guan, Y.-Y.; Jiang, Y.-X.; Wu, Y.; Rahman, K.; Zhang, L.-J.; Liu, H.-J.; Luan, X. Mesoporous silica nanoparticles: Facile surface functionalization and versatile biomedical applications in oncology. *Acta Biomater.* **2020**, *116*, 1–15. [CrossRef]
51. Song, S.W.; Hidajat, K.; Kawi, S. Functionalized SBA-15 Materials as Carriers for Controlled Drug Delivery: Influence of Surface Properties on Matrix-Drug Interactions. *Langmuir* **2005**, *21*, 9568–9575. [CrossRef] [PubMed]
52. Nieto, A.; Colilla, M.; Balas, F.; Vallet-Regí, M. Surface Electrochemistry of Mesoporous Silicas as a Key Factor in the Design of Tailored Delivery Devices. *Langmuir* **2010**, *26*, 5038–5049. [CrossRef] [PubMed]
53. Aguilar-Colomer, A.; Colilla, M.; Izquierdo-Barba, I.; Jiménez-Jiménez, C.; Mahillo, I.; Esteban, J.; Vallet-Regí, M. Impact of the antibiotic-cargo from MSNs on gram-positive and gram-negative bacterial biofilms. *Micropor. Mesopor. Mat.* **2021**, *311*, 110681. [CrossRef]
54. Balas, F.; Manzano, M.; Colilla, M.; Vallet-Regí, M. L-Trp adsorption into silica mesoporous materials to promote bone formation. *Acta Biomater.* **2008**, *4*, 514–522. [CrossRef]
55. González, B.; Colilla, M.; Díez, J.; Pedraza, D.; Guembe, M.; Izquierdo-Barba, I.; Vallet-Regí, M. Mesoporous silica nanoparticles decorated with polycationic dendrimers for infection treatment. *Acta Biomater.* **2018**, *68*, 261–271. [CrossRef]
56. Pedraza, D.; Díez, J.; Isabel Izquierdo, B.; Colilla, M.; Vallet-Regí, M. Amine-Functionalized Mesoporous Silica Nanoparticles: A New Nanoantibiotic for Bone Infection Treatment. *Biomed. Glass.* **2018**, *4*, 1–12. [CrossRef]
57. Encinas, N.; Angulo, M.; Astorga, C.; Colilla, M.; Izquierdo-Barba, I.; Vallet-Regí, M. Mixed-charge pseudo-zwitterionic mesoporous silica nanoparticles with low-fouling and reduced cell uptake properties. *Acta Biomater.* **2019**, *84*, 317–327. [CrossRef]

58. Arca, H.; Mosquera-Giraldo, L.I.; Pereira, J.M.; Sriranganathan, N.; Taylor, L.S.; Edgar, K.J. Rifampin Stability and Solution Concentration Enhancement Through Amorphous Solid Dispersion in Cellulose ω -Carboxyalkanoate Matrices. *J. Pharm. Sci.* **2018**, *107*, 127–138. [[CrossRef](#)]
59. Doadrio, A.L.; Doadrio, J.C.; Sánchez-Montero, J.M.; Salinas, A.J.; Vallet-Regí, M. A rational explanation of the vancomycin release from SBA-15 and its derivative by molecular modelling. *Micropor. Mesopor. Mat.* **2010**, *132*, 559–566. [[CrossRef](#)]
60. Gusev, V.Y.; Feng, X.; Bu, Z.; Haller, G.L.; O'Brien, J.A. Mechanical stability of pure silica mesoporous MCM-41 by nitrogen adsorption and small-angle X-ray diffraction measurements. *J. Phys. Chem.* **1996**, *100*, 1985–1988. [[CrossRef](#)]
61. Doadrio, A.; Salinas, A.; Montero, J.M.; Vallet-Regí, M. Drug Release from Ordered Mesoporous Silicas. *Curr. Pharm. Des.* **2015**, *22*. [[CrossRef](#)]
62. Salviano, A.B.; Santos, M.R.D.; de Araújo, L.M.; Ardisson, J.D.; Lago, R.M.; Araujo, M.H. Iron Oxide Nanoparticles Supported on Mesoporous MCM-41 for Efficient Adsorption of Hazardous β -Lactamic Antibiotics. *Water Air Soil Pollut.* **2018**, *229*, 59. [[CrossRef](#)]
63. Vallet-Regí, M.; Doadrio, J.; Doadrio, A.; Izquierdo-Barba, I.; Pérez-Pariente, J. Hexagonal ordered mesoporous material as a matrix for the controlled release of amoxicillin. *Solid State Ion.* **2004**, *172*, 435–439. [[CrossRef](#)]
64. Pourjavadi, A.; Tehrani, Z.M. Mesoporous silica nanoparticles (MCM-41) coated PEGylated chitosan as a pH-responsive nanocarrier for triggered release of erythromycin. *Int. J. Polym. Mater.* **2014**, *63*, 692–697. [[CrossRef](#)]
65. Orbeci, C.; Stănescu, R.; Negoescu, D.; Parvulescu, V. Synthesis, characterization and functionalization of MCM-41 for the removal of organic compounds from wastewaters. *EEMJ* **2017**, *16*. [[CrossRef](#)]
66. Doadrio, J.C.; Sousa, E.M.; Izquierdo-Barba, I.; Doadrio, A.L.; Perez-Pariente, J.; Vallet-Regí, M. Functionalization of mesoporous materials with long alkyl chains as a strategy for controlling drug delivery pattern. *J. Mater. Chem.* **2006**, *16*, 462–466. [[CrossRef](#)]
67. Izquierdo-Barba, I.; Martínez, Á.; Doadrio, A.L.; Pérez-Pariente, J.; Vallet-Regí, M. Release evaluation of drugs from ordered three-dimensional silica structures. *Eur. J. Pharm. Sci.* **2005**, *26*, 365–373. [[CrossRef](#)]
68. Tariq, S.; Rahim, A.; Muhammad, N.; Rahman, S.U.; Azhar, U.; Sultana, K.; Sharif, F.; Siddiqi, S.A.; Zaman, M.; Rehman, F. Controllable delivery from gentamicin loaded polycaprolactone/grafted silica nanoparticles composite mats. *J. Mol. Liq.* **2019**, *290*, 111205. [[CrossRef](#)]
69. Doadrio, A.; Sousa, E.; Doadrio, J.; Pariente, J.P.; Izquierdo-Barba, I.; Vallet-Regí, M. Mesoporous SBA-15 HPLC evaluation for controlled gentamicin drug delivery. *J. Control. Release* **2004**, *97*, 125–132. [[CrossRef](#)]
70. Jin, T.; Yuan, W.; Xue, Y.; Wei, H.; Zhang, C.; Li, K. Co-modified MCM-41 as an effective adsorbent for levofloxacin removal from aqueous solution: Optimization of process parameters, isotherm, and thermodynamic studies. *Environ. Sci. Pollut. Res.* **2017**, *24*, 5238–5248. [[CrossRef](#)] [[PubMed](#)]
71. Siafaka, P.; Okur, M.E.; Ayla, Ş.; Er, S.; Çağlar, E.Ş.; Okur, N.Ü. Design and characterization of nanocarriers loaded with Levofloxacin for enhanced antimicrobial activity; physicochemical properties, in vitro release and oral acute toxicity. *Braz. J. Pharm. Sci.* **2019**, *55*. [[CrossRef](#)]
72. Adristya, I.; Suryaningtyas, A.D.; Wijaya, J.; Pangestu, F.C.; Hartono, S.B.; Soewignyo, L.; Irawaty, W. Mesoporous silica nanoparticles as vehicles for drug delivery. In *IOP Conference Series: Materials Science and Engineering*; IOP Publishing: Bristol, UK, 2020; p. 012021.
73. Wu, S.; Huang, Y.; Yan, J.; Li, Y.; Wang, J.; Yang, Y.Y.; Yuan, P.; Ding, X. Bacterial Outer Membrane-Coated Mesoporous Silica Nanoparticles for Targeted Delivery of Antibiotic Rifampicin against Gram-Negative Bacterial Infection In Vivo. *Adv. Funct. Mater.* **2021**, *31*, 2103442. [[CrossRef](#)]
74. Doadrio, A.L.; Sánchez-Montero, J.M.; Doadrio, J.C.; Salinas, A.J.; Vallet-Regí, M. Mesoporous silica nanoparticles as a new carrier methodology in the controlled release of the active components in a polypill. *Eur. J. Pharm. Sci.* **2017**, *97*, 1–8. [[CrossRef](#)]
75. Jijie, R.; Barras, A.; Teodorescu, F.; Boukherroub, R.; Szunerits, S. Advancements on the molecular design of nanoantibiotics: Current level of development and future challenges. *Mol. Syst. Des. Eng.* **2017**, *2*, 349–369. [[CrossRef](#)]
76. Castillo, R.R.; Lozano, D.; González, B.; Manzano, M.; Izquierdo-Barba, I.; Vallet-Regí, M. Advances in mesoporous silica nanoparticles for targeted stimuli-responsive drug delivery: An update. *Expert Opin. Drug Deliv.* **2019**, *16*, 415–439. [[CrossRef](#)]
77. Vallet-Regí, M.; Colilla, M.; Izquierdo-Barba, I. Drug Delivery and Bone Infection. *Enzymes* **2018**, *44*, 35–59. [[CrossRef](#)]
78. Zeng, M.; Shu, Y.; Parra-Robert, M.; Desai, D.; Zhou, H.; Li, Q.; Rong, Z.; Karaman, D.; Yang, H.; Peng, J.; et al. Scalable synthesis of multicomponent multifunctional inorganic core@mesoporous silica shell nanocomposites. *Mater. Sci. Eng. C Mater. Biol. Appl.* **2021**, *128*, 112272. [[CrossRef](#)]
79. Castillo, R.R.; de la Torre, L.; García-Ochoa, F.; Ladero, M.; Vallet-Regí, M. Production of MCM-41 Nanoparticles with Control of Particle Size and Structural Properties: Optimizing Operational Conditions during Scale-Up. *Int. J. Mol. Sci.* **2020**, *21*, 7899. [[CrossRef](#)]
80. Aragonese-Cazorla, G.; Serrano-Lopez, J.; Martinez-Alfonzo, I.; Vallet-Regí, M.; González, B.; Luque-Garcia, J.L. A novel hemocompatible core@shell nanosystem for selective targeting and apoptosis induction in cancer cells. *Inorg. Chem. Front.* **2021**, *8*, 2697–2712. [[CrossRef](#)]
81. Clemens, D.L.; Lee, B.-Y.; Xue, M.; Thomas, C.R.; Meng, H.; Ferris, D.; Nel, A.E.; Zink, J.I.; Horwitz, M.A. Targeted intracellular delivery of antituberculosis drugs to mycobacterium tuberculosis-infected macrophages via functionalized mesoporous silica nanoparticles. *Antimicrob. Agents Chemother.* **2012**, *56*, 2535–2545. [[CrossRef](#)]
82. Hwang, A.A.; Lee, B.-Y.; Clemens, D.L.; Dillon, B.J.; Zink, J.I.; Horwitz, M.A. pH-Responsive Isoniazid-Loaded Nanoparticles Markedly Improve Tuberculosis Treatment in Mice. *Small* **2015**, *11*, 5066–5078. [[CrossRef](#)]

83. Montalvo-Quirós, S.; Gómez-Graña, S.; Vallet-Regí, M.; Prados-Rosales, R.C.; González, B.; Luque-García, J.L. Mesoporous silica nanoparticles containing silver as novel antimycobacterial agents against *Mycobacterium tuberculosis*. *Colloids Surf. B Biointerfaces* **2021**, *197*, 111405. [[CrossRef](#)]
84. Beitzinger, B.; Gerbl, F.; Vomhof, T.; Schmid, R.; Noschka, R.; Rodriguez, A.; Wiese, S.; Weidinger, G.; Ständker, L.; Walther, P.; et al. Delivery by Dendritic Mesoporous Silica Nanoparticles Enhances the Antimicrobial Activity of a Napsin-Derived Peptide Against Intracellular *Mycobacterium tuberculosis*. *Adv. Healthc. Mater.* **2021**, *10*, e2100453. [[CrossRef](#)]
85. Navarre, W.W.; Schneewind, O. Surface proteins of gram-positive bacteria and mechanisms of their targeting to the cell wall envelope. *Microbiol. Mol. Biol. Rev.* **1999**, *63*, 174–229. [[CrossRef](#)]
86. Beveridge, T.J. Structures of gram-negative cell walls and their derived membrane vesicles. *J. Bacteriol.* **1999**, *181*, 4725–4733. [[CrossRef](#)]
87. Ruehle, B.; Clemens, D.L.; Lee, B.-Y.; Horwitz, M.A.; Zink, J.I. A Pathogen-Specific Cargo Delivery Platform Based on Mesoporous Silica Nanoparticles. *J. Am. Chem. Soc.* **2017**, *139*, 6663–6668. [[CrossRef](#)]
88. Xu, T.; Li, J.; Zhang, S.; Jin, Y.; Wang, R. Integration of diagnosis and treatment in the detection and kill of *S.aureus* in the whole blood. *Biosens. Bioelectron.* **2019**, *142*, 111507. [[CrossRef](#)]
89. Kavruk, M.; Celikbicak, O.; Ozalp, V.C.; Borsa, B.A.; Hernandez, F.J.; Bayramoglu, G.; Salih, B.; Arica, M.Y. Antibiotic loaded nanocapsules functionalized with aptamer gates for targeted destruction of pathogens. *Chem. Commun.* **2015**, *51*, 8492–8495. [[CrossRef](#)]
90. Yang, S.; Han, X.; Yang, Y.; Qiao, H.; Yu, Z.; Liu, Y.; Wang, J.; Tang, T. Bacteria-Targeting Nanoparticles with Microenvironment-Responsive Antibiotic Release To Eliminate Intracellular *Staphylococcus aureus* and Associated Infection. *ACS Appl. Mater. Interfaces* **2018**, *10*, 14299–14311. [[CrossRef](#)]
91. Rathnayake, K.; Patel, U.; Pham, C.; McAlpin, A.; Budisalih, T.; Jayawardana, S.N. Targeted Delivery of Antibiotic Therapy to Inhibit *Pseudomonas aeruginosa* Using Lipid-Coated Mesoporous Silica Core-Shell Nanoassembly. *ACS Appl. Bio. Mater.* **2020**, *3*, 6708–6721. [[CrossRef](#)]
92. Hao, N.; Chen, X.; Jeon, S.; Yan, M. Carbohydrate-Conjugated Hollow Oblate Mesoporous Silica Nanoparticles as Nanoantibiotics to Target *Mycobacteria*. *Adv. Healthc. Mater.* **2015**, *4*, 2797–2801. [[CrossRef](#)]
93. Zhou, J.; Jayawardana, K.W.; Kong, N.; Ren, Y.; Hao, N.; Yan, M.; Ramström, O. Trehalose-Conjugated, Photofunctionalized Mesoporous Silica Nanoparticles for Efficient Delivery of Isoniazid into *Mycobacteria*. *ACS Biomater. Sci. Eng.* **2015**, *1*, 1250–1255. [[CrossRef](#)]
94. Mudakavi, R.J.; Vanamali, S.; Chakravorty, D.; Raichur, A.M. Development of arginine based nanocarriers for targeting and treatment of intracellular *Salmonella*. *RSC Adv.* **2017**, *7*, 7022–7032. [[CrossRef](#)]
95. Chen, X.; Liu, Y.; Lin, A.; Huang, N.; Long, L.; Gang, Y.; Liu, J. Folic acid-modified mesoporous silica nanoparticles with pH-responsiveness loaded with Amp for an enhanced effect against anti-drug-resistant bacteria by overcoming efflux pump systems. *Biomater. Sci.* **2018**, *6*, 1923–1935. [[CrossRef](#)] [[PubMed](#)]
96. Qi, G.; Li, L.; Yu, F.; Wang, H. Vancomycin-Modified Mesoporous Silica Nanoparticles for Selective Recognition and Killing of Pathogenic Gram-Positive Bacteria Over Macrophage-Like Cells. *ACS Appl. Mater. Interfaces* **2013**, *5*, 10874–10881. [[CrossRef](#)] [[PubMed](#)]
97. Lesniak, A.; Salvati, A.; Santos-Martinez, M.J.; Radomski, M.W.; Dawson, K.A.; Åberg, C. Nanoparticle Adhesion to the Cell Membrane and Its Effect on Nanoparticle Uptake Efficiency. *J. Am. Chem. Soc.* **2013**, *135*, 1438–1444. [[CrossRef](#)]
98. Häffner, S.M.; Parra-Ortiz, E.; Browning, K.L.; Jørgensen, E.; Skoda, M.W.; Montis, C.; Li, X.; Berti, D.; Zhao, D.; Malmsten, M. Membrane Interactions of Virus-like Mesoporous Silica Nanoparticles. *ACS Nano* **2021**, *15*, 6787–6800. [[CrossRef](#)]
99. Wang, P.; Jiang, S.; Li, Y.; Luo, Q.; Lin, J.; Hu, L.; Liu, X.; Xue, F. Virus-like mesoporous silica-coated plasmonic Ag nanocube with strong bacteria adhesion for diabetic wound ulcer healing. *Nanomed. Nanotechnol. Biol. Med.* **2021**, *34*, 102381. [[CrossRef](#)]
100. Bandyopadhyay, A.; McCarthy, K.A.; Kelly, M.A.; Gao, J. Targeting bacteria via iminoboronate chemistry of amine-presenting lipids. *Nat. Commun.* **2015**, *6*, 6561. [[CrossRef](#)]
101. Lam, S.J.; O'Brien-Simpson, N.M.; Pantarat, N.; Sulistio, A.; Wong, E.H.H.; Chen, Y.-Y.; Lenzo, J.C.; Holden, J.A.; Blencowe, A.; Reynolds, E.C.; et al. Combating multidrug-resistant Gram-negative bacteria with structurally nanoengineered antimicrobial peptide polymers. *Nat. Microbiol.* **2016**, *1*, 16162. [[CrossRef](#)]
102. Radovic-Moreno, A.F.; Lu, T.K.; Puscasu, V.A.; Yoon, C.J.; Langer, R.; Farokhzad, O.C. Surface Charge-Switching Polymeric Nanoparticles for Bacterial Cell Wall-Targeted Delivery of Antibiotics. *ACS Nano* **2012**, *6*, 4279–4287. [[CrossRef](#)]
103. Ruiz-Rico, M.; Pérez-Esteve, É.; de la Torre, C.; Jiménez-Belenguer, A.I.; Quiles, A.; Marcos, M.D.; Martínez-Mañez, R.; Barat, J.M. Improving the Antimicrobial Power of Low-Effective Antimicrobial Molecules Through Nanotechnology. *J. Food Sci.* **2018**, *83*, 2140–2147. [[CrossRef](#)]
104. Mas, N.; Galiana, I.; Mondragón, L.; Aznar, E.; Climent, E.; Cabedo, N.; Sancenón, F.; Murguía, J.R.; Martínez-Mañez, R.; Marcos, M.D.; et al. Enhanced Efficacy and Broadening of Antibacterial Action of Drugs via the Use of Capped Mesoporous Nanoparticles. *Chem. Eur. J.* **2013**, *19*, 11167–11171. [[CrossRef](#)]
105. Velikova, N.; Mas, N.; Miguel-Romero, L.; Polo, L.; Stolte, E.; Zaccaria, E.; Cao, R.; Taverne, N.; Murguía, J.R.; Martínez-Manez, R.; et al. Broadening the antibacterial spectrum of histidine kinase autophosphorylation inhibitors via the use of ϵ -poly-L-lysine capped mesoporous silica-based nanoparticles. *Nanomed. Nanotechnol. Biol. Med.* **2017**, *13*, 569–581. [[CrossRef](#)]
106. Mah, T.F.; O'Toole, G.A. Mechanisms of biofilm resistance to antimicrobial agents. *Trends Microbiol.* **2001**, *9*, 34–39. [[CrossRef](#)]

107. Jefferson, K.K. What drives bacteria to produce a biofilm? *FEMS Microbiol. Lett.* **2004**, *236*, 163–173. [[CrossRef](#)]
108. Xu, C.; He, Y.; Li, Z.; Ahmad Nor, Y.; Ye, Q. Nanoengineered hollow mesoporous silica nanoparticles for the delivery of antimicrobial proteins into biofilms. *J. Mater. Chem. B* **2018**, *6*, 1899–1902. [[CrossRef](#)]
109. Tasia, W.; Lei, C.; Cao, Y.; Ye, Q.; He, Y.; Xu, C. Enhanced eradication of bacterial biofilms with DNase I-loaded silver-doped mesoporous silica nanoparticles. *Nanoscale* **2020**, *12*, 2328–2332. [[CrossRef](#)]
110. Fulaz, S.; Devlin, H.; Vitale, S.; Quinn, L.; O’Gara, J.P.; Casey, E. Tailoring Nanoparticle-Biofilm Interactions to Increase the Efficacy of Antimicrobial Agents Against *Staphylococcus aureus*. *Int. J. Nanomed.* **2020**, *15*, 4779–4791. [[CrossRef](#)]
111. Martínez-Carmona, M.; Izquierdo-Barba, I.; Colilla, M.; Vallet-Regí, M. Concanavalin A-targeted mesoporous silica nanoparticles for infection treatment. *Acta Biomater.* **2019**, *96*, 547–556. [[CrossRef](#)]
112. Aguilera-Correa, J.J.; Gisbert-Garzarán, M.; Mediero, A.; Carias-Cálix, R.A.; Jiménez-Jiménez, C.; Esteban, J.; Vallet-Regí, M. Arabic gum plus colistin coated moxifloxacin-loaded nanoparticles for the treatment of bone infection caused by *Escherichia coli*. *Acta Biomater.* **2021**. [[CrossRef](#)]
113. Gounani, Z.; Asadollahi, M.A.; Pedersen, J.N.; Lyngsø, J.; Pedersen, J.S.; Arpanaei, A.; Meyer, R.L. Mesoporous silica nanoparticles carrying multiple antibiotics provide enhanced synergistic effect and improved biocompatibility. *Colloids Surf. B Biointerfaces.* **2019**, *175*, 498–508. [[CrossRef](#)]
114. Mebert, A.M.; Aimé, C.; Álvarez, G.S.; Shi, Y.; Flor, S.A.; Lucangioli, S.I.; Desimone, M.F.; Coradin, T. Silica core-shell particles for the dual delivery of gentamicin and rifamycin antibiotics. *J. Mater. Chem. B* **2016**, *4*, 3135–3144. [[CrossRef](#)] [[PubMed](#)]
115. Cheng, Y.; Zhang, Y.; Deng, W.; Hu, J. Antibacterial and anticancer activities of asymmetric lollipop-like mesoporous silica nanoparticles loaded with curcumin and gentamicin sulfate. *Colloids Surf. B Biointerfaces* **2020**, *186*, 110744. [[CrossRef](#)] [[PubMed](#)]
116. Zhu, X.; Radovic-Moreno, A.F.; Wu, J.; Langer, R.; Shi, J. Nanomedicine in the management of microbial infection—Overview and perspectives. *Nano Today* **2014**, *9*, 478–498. [[CrossRef](#)] [[PubMed](#)]
117. Perelshtein, I.; Lipovsky, A.; Perkas, N.; Gedanken, A.; Moschini, E.; Mantecca, P. The influence of the crystalline nature of nano-metal oxides on their antibacterial and toxicity properties. *Nano Res.* **2015**, *8*, 695–707. [[CrossRef](#)]
118. Ong, C.; Lim, J.Z.Z.; Ng, C.T.; Li, J.J.; Yung, L.Y.L.; Bay, B.H. Silver Nanoparticles in Cancer: Therapeutic Efficacy and Toxicity. *Curr. Med. Chem.* **2013**, *20*, 772–781. [[CrossRef](#)]
119. AshaRani, P.V.; Low Kah Mun, G.; Hande, M.P.; Valiyaveetil, S. Cytotoxicity and Genotoxicity of Silver Nanoparticles in Human Cells. *ACS Nano* **2009**, *3*, 279–290. [[CrossRef](#)]
120. Fernández, M.N.; Muñoz-Olivas, R.; Luque-García, J.L. SILAC-based quantitative proteomics identifies size-dependent molecular mechanisms involved in silver nanoparticles-induced toxicity. *Nanotoxicology* **2019**, *13*, 812–826. [[CrossRef](#)]
121. Li, Y.; Yang, L.; Zhao, Y.; Li, B.; Sun, L.; Luo, H. Preparation of AgBr@SiO₂ core@shell hybrid nanoparticles and their bactericidal activity. *Mater. Sci. Eng. C Mater. Biol. Appl.* **2013**, *33*, 1808–1812. [[CrossRef](#)]
122. Montalvo-Quiros, S.; Aragonese-Cazorla, G.; Garcia-Alcalde, L.; Vallet-Regí, M.; González, B.; Luque-García, J.L. Cancer cell targeting and therapeutic delivery of silver nanoparticles by mesoporous silica nanocarriers: Insights into the action mechanisms using quantitative proteomics. *Nanoscale* **2019**, *11*, 4531–4545. [[CrossRef](#)]
123. Wang, Y.; Ding, X.; Chen, Y.; Guo, M.; Zhang, Y.; Guo, X.; Gu, H. Antibiotic-loaded, silver core-embedded mesoporous silica nanovehicles as a synergistic antibacterial agent for the treatment of drug-resistant infections. *Biomaterials* **2016**, *101*, 207–216. [[CrossRef](#)]
124. Tian, Y.; Qi, J.; Zhang, W.; Cai, Q.; Jiang, X. Facile, One-Pot Synthesis, and Antibacterial Activity of Mesoporous Silica Nanoparticles Decorated with Well-Dispersed Silver Nanoparticles. *ACS Appl. Mater. Interfaces* **2014**, *6*, 12038–12045. [[CrossRef](#)]
125. Liong, M.; France, B.; Bradley, K.A.; Zink, J.I. Antimicrobial activity of silver nanocrystals encapsulated in mesoporous silica nanoparticles. *Adv. Mater.* **2009**, *21*, 1684–1689. [[CrossRef](#)]
126. Chang, Z.-M.; Wang, Z.; Lu, M.M.; Shao, D.; Yue, J.; Yang, D.; Li, M.-Q.; Dong, W.-F. Janus silver mesoporous silica nanobullets with synergistic antibacterial functions. *Colloids Surf. B Biointerfaces* **2017**, *157*, 199–206. [[CrossRef](#)]
127. Song, Y.; Cai, L.; Tian, Z.; Wu, Y. Phytochemical Curcumin-Coformulated, Silver-Decorated Melanin-like Polydopamine/Mesoporous Silica Composites with Improved Antibacterial and Chemotherapeutic Effects against Drug-Resistant Cancer Cells. *ACS Omega* **2020**, *5*, 15083–15094. [[CrossRef](#)]
128. Álvarez, E.; Estévez, M.; Jiménez-Jiménez, C.; Colilla, M.; Izquierdo-Barba, I.; González, B.; Vallet-Regí, M. A versatile multicomponent mesoporous silica nanosystem with dual antimicrobial and osteogenic effects. *Acta Biomater.* **2021**, *136*, 570–581. [[CrossRef](#)]
129. Aguilera-Correa, J.J.; Esteban, J.; Vallet-Regí, M. Inorganic and Polymeric Nanoparticles for Human Viral and Bacterial Infections Prevention and Treatment. *Nanomaterials* **2021**, *11*, 137. [[CrossRef](#)]
130. Wen, J.; Yang, K.; Liu, F.; Li, H.; Xu, Y.; Sun, S. Diverse gatekeepers for mesoporous silica nanoparticle based drug delivery systems. *Chem. Soc. Rev.* **2017**, *46*, 6024–6045. [[CrossRef](#)]
131. Karimi, M.; Ghasemi, A.; Zangabad, P.S.; Rahighi, R.; Basri, S.M.M.; Mirshekari, H.; Amiri, M.; Pishabad, Z.S.; Aslani, A.; Bozorgomid, M.; et al. Smart micro/nanoparticles in stimulus-responsive drug/gene delivery systems. *Chem. Soc. Rev.* **2016**, *45*, 1457–1501. [[CrossRef](#)]
132. Yu, M.; Gu, Z.; Ottewill, T.; Yu, C. Silica-based nanoparticles for therapeutic protein delivery. *J. Mater. Chem. B* **2017**, *5*, 3241–3252. [[CrossRef](#)]
133. Vallet-Regí, M.; Colilla, M.; Izquierdo-Barba, I. Bioactive Mesoporous Silicas as Controlled Delivery Systems: Application in Bone Tissue Regeneration. *J. Biomed. Nanotechnol.* **2008**, *4*, 1–15. [[CrossRef](#)]

134. Villaverde, G.; Alfranca, A.; Gonzalez-Murillo, Á.; Melen, G.J.; Castillo, R.R.; Ramírez, M.; Baeza, A.; Vallet-Regí, M. Molecular Scaffolds as Double-Targeting Agents for the Diagnosis and Treatment of Neuroblastoma. *Angew. Chem. Int. Ed.* **2019**, *58*, 3067–3072. [[CrossRef](#)]
135. Mora-Raimundo, P.; Lozano, D.; Manzano, M.; Vallet-Regí, M. Nanoparticles to Knockdown Osteoporosis-Related Gene and Promote Osteogenic Marker Expression for Osteoporosis Treatment. *ACS Nano* **2019**, *13*, 5451–5464. [[CrossRef](#)]
136. Mora-Raimundo, P.; Lozano, D.; Benito, M.; Mulero, F.; Manzano, M.; Vallet-Regí, M. Osteoporosis Remission and New Bone Formation with Mesoporous Silica Nanoparticles. *Adv. Sci.* **2021**, *8*, 2101107. [[CrossRef](#)]
137. Chen, Y.; Zhang, H.; Cai, X.; Ji, J.; He, S.; Zhai, G. Multifunctional mesoporous silica nanocarriers for stimuli-responsive target delivery of anticancer drugs. *RSC Adv.* **2016**, *6*, 92073–92091. [[CrossRef](#)]
138. Lemichez, E.; Barbieri, J.T. General aspects and recent advances on bacterial protein toxins. *Cold Spring Harb. Perspect. Med.* **2013**, *3*, a013573. [[CrossRef](#)]
139. Lee, B.Y.; Li, Z.; Clemens, D.L.; Dillon, B.J.; Hwang, A.A.; Zink, J.I.; Horwitz, M.A. Redox-Triggered Release of Moxifloxacin from Mesoporous Silica Nanoparticles Functionalized with Disulfide Snap-Tops Enhances Efficacy Against Pneumonic Tularemia in Mice. *Small* **2016**, *12*, 3690–3702. [[CrossRef](#)]
140. Tsujimoto, H.; Ha, D.-G.; Markopoulos, G.; Chae, H.S.; Baldo, M.A.; Swager, T.M. Thermally Activated Delayed Fluorescence and Aggregation Induced Emission with Through-Space Charge Transfer. *J. Am. Chem. Soc.* **2017**, *139*, 4894–4900. [[CrossRef](#)]
141. Liu, Y.; Liu, X.; Xiao, Y.; Chen, F.; Xiao, F. A multifunctional nanoplatfrom based on mesoporous silica nanoparticles for imaging-guided chemo/photodynamic synergetic therapy. *RSC Adv.* **2017**, *7*, 31133–31141. [[CrossRef](#)]
142. Sun, J.; Fan, Y.; Zhang, P.; Zhang, X.; Zhou, Q.; Zhao, J.; Ren, L. Self-enriched mesoporous silica nanoparticle composite membrane with remarkable photodynamic antimicrobial performances. *J. Colloid Interface Sci.* **2020**, *559*, 197–205. [[CrossRef](#)] [[PubMed](#)]
143. Martínez-Carmona, M.; Vallet-Regí, M. Advances in Laser Ablation Synthesized Silicon-Based Nanomaterials for the Prevention of Bacterial Infection. *Nanomaterials* **2020**, *10*, 1443. [[CrossRef](#)] [[PubMed](#)]
144. Ding, Y.; Hao, Y.; Yuan, Z.; Tao, B.; Chen, M.; Lin, C.; Liu, P.; Cai, K. A dual-functional implant with an enzyme-responsive effect for bacterial infection therapy and tissue regeneration. *Biomater. Sci.* **2020**, *8*, 1840–1854. [[CrossRef](#)]
145. Lu, M.M.; Ge, Y.; Qiu, J.; Shao, D.; Zhang, Y.; Bai, J.; Zheng, X.; Chang, Z.M.; Wang, Z.; Dong, W.F.; et al. Redox/pH dual-controlled release of chlorhexidine and silver ions from biodegradable mesoporous silica nanoparticles against oral biofilms. *Int. J. Nanomed.* **2018**, *13*, 7697–7709. [[CrossRef](#)]
146. Fuchs, S.; Pané-Farré, J.; Kohler, C.; Hecker, M.; Engelmann, S. Anaerobic Gene Expression in *Staphylococcus aureus*. *J. Bacteriol.* **2007**, *189*, 4275–4289. [[CrossRef](#)]
147. Bistrian, B. Systemic response to inflammation. *Nutr. Rev.* **2007**, *65*, S170–S172. [[CrossRef](#)]
148. Simmen, H.P.; Blaser, J. Analysis of pH and pO₂ in abscesses, peritoneal fluid, and drainage fluid in the presence or absence of bacterial infection during and after abdominal surgery. *Am. J. Surg.* **1993**, *166*, 24–27. [[CrossRef](#)]
149. Ribeiro, M.; Monteiro, F.J.; Ferraz, M.P. Infection of orthopedic implants with emphasis on bacterial adhesion process and techniques used in studying bacterial-material interactions. *Biomater* **2012**, *2*, 176–194. [[CrossRef](#)]
150. Gisbert-Garzarán, M.; Manzano, M.; Vallet-Regí, M. pH-Responsive Mesoporous Silica and Carbon Nanoparticles for Drug Delivery. *Bioengineering* **2017**, *4*, 3. [[CrossRef](#)]
151. Gisbert-Garzarán, M.; Lozano, D.; Vallet-Regí, M.; Manzano, M. Self-immolative polymers as novel pH-responsive gate keepers for drug delivery. *RSC Adv.* **2017**, *7*, 132–136. [[CrossRef](#)]
152. Martínez-Carmona, M.; Lozano, D.; Colilla, M.; Vallet-Regí, M. Lectin-conjugated pH-responsive mesoporous silica nanoparticles for targeted bone cancer treatment. *Acta Biomater.* **2018**, *65*, 393–404. [[CrossRef](#)]
153. Martínez-Carmona, M.; Ho, Q.P.; Morand, J.; García, A.; Ortega, E.; Erthal, L.C.S.; Ruiz-Hernandez, E.; Santana, M.D.; Ruiz, J.; Vallet-Regí, M.; et al. Amino-Functionalized Mesoporous Silica Nanoparticle-Encapsulated Octahedral Organoruthenium Complex as an Efficient Platform for Combatting Cancer. *Inorg. Chem.* **2020**, *59*, 10275–10284. [[CrossRef](#)]
154. Gisbert-Garzarán, M.; Lozano, D.; Matsumoto, K.; Komatsu, A.; Manzano, M.; Tamanoi, F.; Vallet-Regí, M. Designing Mesoporous Silica Nanoparticles to Overcome Biological Barriers by Incorporating Targeting and Endosomal Escape. *ACS Appl. Mater. Interfaces* **2021**, *13*, 9656–9666. [[CrossRef](#)]
155. Paris, J.L.; de la Torre, P.; Cabañas, M.V.; Manzano, M.; Flores, A.I.; Vallet-Regí, M. Suicide-gene transfection of tumor-tropic placental stem cells employing ultrasound-responsive nanoparticles. *Acta Biomater.* **2019**, *83*, 372–378. [[CrossRef](#)]
156. Paris, J.L.; Cabañas, M.V.; Manzano, M.; Vallet-Regí, M. Polymer-Grafted Mesoporous Silica Nanoparticles as Ultrasound-Responsive Drug Carriers. *ACS Nano* **2015**, *9*, 11023–11033. [[CrossRef](#)]
157. Paris, J.L.; Villaverde, G.; Cabañas, M.V.; Manzano, M.; Vallet-Regí, M. From proof-of-concept material to PEGylated and modularly targeted ultrasound-responsive mesoporous silica nanoparticles. *J. Mater. Chem. B* **2018**, *6*, 2785–2794. [[CrossRef](#)]
158. Paris, J.L.; Manzano, M.; Cabañas, M.V.; Vallet-Regí, M. Mesoporous silica nanoparticles engineered for ultrasound-induced uptake by cancer cells. *Nanoscale* **2018**, *10*, 6402–6408. [[CrossRef](#)]
159. Guisasola, E.; Baeza, A.; Talelli, M.; Arcos, D.; Moros, M.; de la Fuente, J.M.; Vallet-Regí, M. Magnetic-Responsive Release Controlled by Hot Spot Effect. *Langmuir* **2015**, *31*, 12777–12782. [[CrossRef](#)]
160. Guisasola, E.; Asín, L.; Beola, L.; de la Fuente, J.M.; Baeza, A.; Vallet-Regí, M. Beyond Traditional Hyperthermia: In Vivo Cancer Treatment with Magnetic-Responsive Mesoporous Silica Nanocarriers. *ACS Appl. Mater. Interfaces* **2018**, *10*, 12518–12525. [[CrossRef](#)]

161. Villaverde, G.; Gómez-Graña, S.; Guisasola, E.; García, I.; Hanske, C.; Liz-Marzán, L.M.; Baeza, A.; Vallet-Regí, M. Targeted Chemo-Photothermal Therapy: A Nanomedicine Approximation to Selective Melanoma Treatment. *Part. Part. Syst. Charact.* **2018**, *35*, 1800148. [[CrossRef](#)]
162. Martínez-Carmona, M.; Lozano, D.; Baeza, A.; Colilla, M.; Vallet-Regí, M. A novel visible light responsive nanosystem for cancer treatment. *Nanoscale* **2017**, *9*, 15967–15973. [[CrossRef](#)] [[PubMed](#)]
163. Villaverde, G.; Nairi, V.; Baeza, A.; Vallet-Regí, M. Double Sequential Encrypted Targeting Sequence: A New Concept for Bone Cancer Treatment. *Chem. Eur. J.* **2017**, *23*, 7174–7179. [[CrossRef](#)] [[PubMed](#)]
164. Paris, J.L.; Villaverde, G.; Gómez-Graña, S.; Vallet-Regí, M. Nanoparticles for multimodal antivasular therapeutics: Dual drug release, photothermal and photodynamic therapy. *Acta Biomater.* **2020**, *101*, 459–468. [[CrossRef](#)] [[PubMed](#)]
165. García, A.; González, B.; Harvey, C.; Izquierdo-Barba, I.; Vallet-Regí, M. Effective reduction of biofilm through photothermal therapy by gold core@shell based mesoporous silica nanoparticles. *Micropor. Mesopor. Mat.* **2021**, *328*, 111489. [[CrossRef](#)]
166. Angelini, T.E.; Roper, M.; Kolter, R.; Weitz, D.A.; Brenner, M.P. *Bacillus subtilis* spreads by surfing on waves of surfactant. *PNAS* **2009**, *106*, 18109–18113. [[CrossRef](#)] [[PubMed](#)]
167. Whitchurch, C.B.; Tolker-Nielsen, T.; Ragas, P.C.; Mattick, J.S. Extracellular DNA required for bacterial biofilm formation. *Science* **2002**, *295*, 1487. [[CrossRef](#)] [[PubMed](#)]
168. Wang, F.; Liu, L.S.; Lau, C.H.; Han Chang, T.J.; Tam, D.Y.; Leung, H.M.; Tin, C.; Lo, P.K. Synthetic α -l-Threose Nucleic Acids Targeting Bcl-2 Show Gene Silencing and in Vivo Antitumor Activity for Cancer Therapy. *ACS Appl. Mater. Interfaces* **2019**, *11*, 38510–38518. [[CrossRef](#)]
169. Levi-Polyachenko, N.; Young, C.; MacNeill, C.; Braden, A.; Argenta, L.; Reid, S. Eradicating group A streptococcus bacteria and biofilms using functionalised multi-wall carbon nanotubes. *Int. J. Hyperth.* **2014**, *30*, 490–501. [[CrossRef](#)]
170. Dong, K.; Ju, E.; Gao, N.; Wang, Z.; Ren, J.; Qu, X. Synergistic eradication of antibiotic-resistant bacteria based biofilms in vivo using a NIR-sensitive nanoplatfrom. *Chem. Commun.* **2016**, *52*, 5312–5315. [[CrossRef](#)]
171. Allan, R.N.; Kelso, M.J.; Rineh, A.; Yepuri, N.R.; Feelisch, M.; Soren, O.; Brito-Mutunayagam, S.; Salib, R.J.; Stoodley, P.; Clarke, S.C.; et al. Cephalosporin-NO-donor prodrug PYRRO-C3D shows β -lactam-mediated activity against *Streptococcus pneumoniae* biofilms. *Nitric Oxide* **2017**, *65*, 43–49. [[CrossRef](#)]